Demonstration of One Cutoff Phase Space Slicing Method: Next-to-Leading Order QCD Corrections to the tW Associated Production in Hadron Collision

Qing-Hong Cao*

Department of Physics and Astronomy,

University of California at Riverside, Riverside, CA 92531, USA

Abstract

We present a detailed calculation of next-to-leading order QCD corrections to the Wt associated production using the one cutoff phase space slicing method. Such QCD corrections have been calculated independently by two groups already, however, a number of differences were found. It is desirable to have a third party calculation to make a crossing check. In this note, we present our complete results of the virtual corrections which are not shown in the literature so far. The numerical comparison will be presented in the forthcoming paper. As a demonstration of the one cutoff phase space slicing method, we also show in details how to organize the color ordered amplitudes and how to slice the soft and collinear phase space regions.

*Electronic address: qcao@ucr.edu

I. INTRODUCTION

Single top production at the hadron collider has been extensively studied in the literature [1, 2, 3, 4, 5, 6, 7, 8, 9, 10, 11, 12, 13, 14, 15, 16, 17, 18, 19, 20, 21, 22, 23, 24, 25, 26]. There are three separate single top quark production processes of interest at the hadron collider, which may be characterized by the virtuality of the W boson (of four momentum q) in the processes. The s-channel process $q\bar{q}' \to W^* \to t\bar{b}$ via a virtual s-channel W boson involves a timelike W boson, $q^2 > (m_t + m_b)^2$, the t-channel process $qb \to q't$ (including $\bar{q}'b \to \bar{q}t$, also referred as W-gluon fusion) involves a spacelike W boson, $q^2 < 0$, and the tW associated production process $bg \to tW^-$ involves an on-shell W boson, $q^2 = m_W^2$. Therefore, these three single top quark production mechanisms probe the charged-current interaction in different q^2 regions and are thus complementary to each other. To improve the theory prediction on the single top production rate, the next-to-leading order (NLO) corrections, at the order of α_s, for these three channels has been carried out in Refs. [27, 28, 29, 30, 31, 32, 33, 34, 35].

The NLO QCD corrections to the tW associated production have been calculated independently by two groups [28, 35], but a number of differences were found. It is desirable to have a third party calculation to make a crossing check. Furthermore, there is no analytic result available in the literature so far. In this note we present a detailed calculation of the NLO QCD corrections to the tW associated production using one cutoff phase space slicing method. The rest of this paper is organized as follows. In Sec. II, we briefly review the method of our calculation. In Sec. III, we present the Born level helicity amplitudes of the tW production. In Sec. IV we present the NLO virtual corrections. In Sec. V we present the calculation of the soft and collinear singularities of the real emission correction using the one cutoff phase space slicing method.

II. SHORT REVIEW OF THE PHASE SLICING METHOD

The construction of a flexible event generator requires the generation of partonic final states with a minimal amount of implicit phase space integration. At the leading order this is trivial, but in the calculation of NLO QCD corrections, one generally encounters both ultraviolet (UV) and infrared (IR) (soft and collinear) divergences. The former divergences

can be removed by proper renormalization of couplings and wave functions. In order to handle the latter divergences, one has to consider both virtual and real corrections and carefully handle the cancellation of divergences between the soft and collinear contributions and the virtual corrections. The soft divergences will cancel according to the Kinoshita-Lee-Nauenberg (KLN) theorem [36, 37], but some collinear divergences remain uncancelled. In the case of considering the initial state partons, one needs to absorb additional collinear divergences to define the NLO parton distribution function of the initial state partons. After that, all the infrared-safe observables will be free of any singularities. To calculate the inclusive production rate, one can use dimensional regularization to regularize divergences and adopt the modified minimal subtraction ($\overline{\rm MS}$) factorization scheme to obtain the total rate. However, owing to the complicated phase space for multi-parton configurations, analytic calculations are in practice impossible for all but the simplest quantities. During the last few years, effective numerical computational techniques have been developed to calculate the fully differential cross section to NLO and above. There are, broadly speaking, two types of algorithm used for NLO calculations, differing in how they approximate the phase space and matrix elements in the neighborhood of divergent regions:

1. The phase space slicing (PSS) method is based on approximating the matrix elements and the phase space integration measure in boundary regions of phase space so integration may be carried out analytically [38, 39, 40, 41, 42, 43].

2. The subtraction method is based on adding and subtracting counterterms designed to approximate the real emission amplitudes in the phase space boundary regions on the one hand, and to be integrable with respect to the momentum of an unresolved parton on the other [44, 45, 46, 47, 48, 49, 50].

The phase space slicing method makes use of a combination of analytic and Monte Carlo integration methods, which has many advantages over a purely analytic calculation. The Monte Carlo approach allows one to calculate any number of observables simultaneously by simply histogramming the appropriate quantities. Furthermore, it is easy to tailor the Monte Carlo calculation to different experimental conditions, for example, detector acceptances, experimental cuts, and jet definitions. Also, with the Monte Carlo approach one can study the dependence of the cross section on the choice of scale and the size of higher order

quantum corrections in different regions of phase space. The basic challenge is to design a program which retains the versatility inherent in a Monte Carlo approach while ensuring that all of the required cancellations of singularities still take place.

In this study, we use the phase space slicing method with one cutoff scale for which the universal crossing functions have been derived in Refs. [41, 42, 43]. The advantage of this method is that, after calculating the effective matrix elements with all the partons in the final state, we can use the generalized crossing property of the NLO matrix elements to calculate the corresponding matrix elements numerically without requiring any further effort. The validity of this method is due to the property that both the phase space and matrix element for the initial and final state collinear radiation processes can be simultaneously factorized. Below, we briefly review the general formalism for the NLO calculation in PSS method with one cutoff scale.

The phase space slicing method with one cutoff scale introduces an unphysical parameter $s_{\min}$ to separate the real emission correction phase space into two regions:

1. the resolved region in which the amplitude has no divergences and can be integrated numerically by Monte Carlo method;

2. unresolved region in which the amplitude contains all the soft and collinear divergences and can be integrated out analytically.

It should be emphasized that the notion of resolved/unresolved partons is unrelated to the physical jet resolution criterium or to any other relevant physical scale. In the massless case, a convenient definition of the resolved region is given by the requirement

$$s_{ij} = (p_i + p_j)^2 > s_{min}, \tag{1}$$

for all invariants $s_{ij} = (p_i + p_j)^2$, where p_i and p_j are the 4-momenta of partons i and j, respectively. For the massive quarks, we follow the definition in Ref. [51] to account for masses, but still use the terminology "resolved" and "unresolved" partons. In the regions with unresolved partons, soft and collinear approximations of the matrix elements, which hold exactly in the limit $s_{min} \to 0$, are used. The necessary integrations over the soft and collinear regions of phase space can then be carried out analytically in $d = 4 - 2\epsilon$ space-time dimensions. One can thus isolate all the poles in ϵ and perform the cancellation

of the IR singularities between the real and virtual contributions and absorb the leftover singularities into the parton structure functions in the factorization procedure. After the above procedure, one takes the limit $\epsilon \to 0$. The contribution from the sum of virtual and unresolved region corrections is finite but s_{min} dependent. Since the parameter s_{min} is introduced in the theoretical calculation for technical reasons only and is unrelated to any physical quantity, the sum of all contributions (virtual, unresolved and resolved corrections) must not depend on s_{min}. The phase space slicing method is only valid in the limit that $s_{\rm min}$ is small enough that a given jet finding algorithm (or any infrared-safe observable) can be consistently defined even after including the experimental cuts.

In general, the conventional calculation of the NLO differential cross section for a process with initial state hadrons H_1 and H_2 can be written as

$$d\sigma^{NLO}_{H_1H_2} = \sum_{a,b} \int dx_1 dx_2 f_a^{H_1}(x_1,\mu_F) f_b^{H_2}(x_2,\mu_F) d\widehat{\sigma^{NLO}_{ab}}(x_{1,}x_2,\mu_R), \tag{2}$$

where a, b denote parton flavors and x_1,x_2 are parton momentum fractions. $f_a^H(x,\mu_F)$ is the usual NLO parton distribution function with the mass factorization scale μ_F and $d\widehat{\sigma^{NLO}_{ab}}(x_1,x_2,\mu_R)$ is the NLO hard scattering differential cross section with the renormalization scale μ_R. The pictorial demonstration of Eq. (2) is shown in the upper part of Fig. 1.

Contrary to the conventional calculation method, the PSS method with one cutoff scale will firstly cross the initial state partons into the final state, including the virtual corrections and unresolved real emission corrections. For example, to calculate the NLO QCD correction to the W-boson production via the Drell-Yan process, we first calculate the radiative corrections to $W \to q\bar{q}'(g)$, as shown in the lower part of the Fig. 1, in which we split the phase space of the real emission corrections into the unresolved and resolved region. After we integrate out the unresolved phase space region, the net contribution of the virtual corrections and the real emission corrections in the unresolved phase space is finite but theoretical cutoff s_{min} dependent, which can be written as a form factor (denoted by the box in Fig. 1) of the Born level vertex.

Secondly, we take the already calculated effective matrix elements with all the partons in the final state and use the universal "crossing function", which is the generalization of the crossing property of the LO matrix elements to NLO, to calculate the corresponding matrix elements numerically. Once we cross the needed partons to the initial state, the

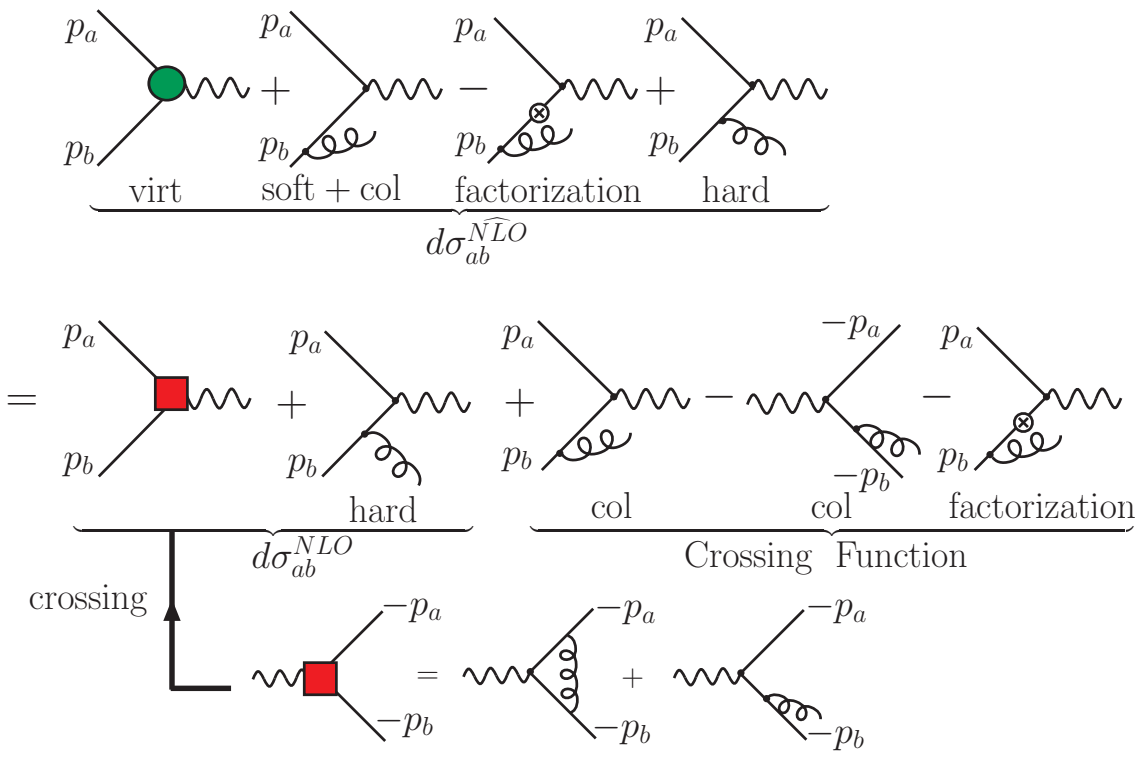

FIG. 1: Illustration of the PSS method with one cutoff scale to describe the processes with initial state massless quarks. Here, only half of the real emission diagrams is shown. In this paper, we will assign the particle's momentum such that the initial state particle's momentum is incoming to the vertex while the final state particle's momentum is outgoing.

contributions from the unresolved collinear phase space regions are different from those with all the partons in the final state. These differences are included into the definition of the crossing function as well as the mass factorization effects, as shown in the middle part of Fig. 1. Here, we only present the explicit expressions of the crossing function, while the definition and detailed derivation of the crossing function can be found in Ref. [42]. After applying the mass factorization in a particular scheme, the crossing functions for an initial state parton a, which participates in the hard scattering processes, can be written in the form:

$$C_a^{\rm scheme}(x,\mu_F,s_{min}) = \left(\frac{N_C}{2\pi}\right)\left[A_a(x,\mu_F)\log\left(\frac{s_{min}}{\mu_F}\right) + B_a^{\rm scheme}(x,\mu_F)\right], \tag{3}$$

where

$$A_a(x,\mu_F) \;=\; \sum_p A_{p\to a}\left(x,\mu_F\right), \tag{4}$$

$$B_a^{\rm scheme}(x,\mu_F) \;=\; \sum_p B_{p\to a}^{\rm scheme}(x,\mu_F), \tag{5}$$

and N_C denotes the number of colors. The sum runs over $p = q, \bar{q}, g$. The functions A and B can be expressed as convolution integrals over the parton distribution functions and the explicit forms can be found in Ref. [42]. Although A_a is scheme independent, B_a does depend on the mass factorization scheme, and therefore so does the crossing function.

After introducing the crossing function, we can write the NLO differential cross section in the PSS method with one cutoff scale as

$$\begin{aligned} & d\sigma_{H_1H_2}^{NLO} \\ &= \sum_{a,b} \int dx_1 dx_2 f_a^{H_1}(x_1,\mu_F) f_b^{H_2}(x_2,\mu_F) d\sigma_{ab}^{NLO}(x_1,x_2,\mu_R) \\ &+ \; \alpha_s(\mu_R) \left[C_a^{H_1}(x_1,\mu_F) f_b^{H_2}(x_2,\mu_F) + f_a^{H_1}(x_1,\mu_F) C_b^{H_2}(x_2,\mu_F) \right] d\sigma_{ab}^{LO}(x_1,x_2). \end{aligned} \tag{6}$$

Here $d\sigma_{ab}^{NLO}$ consists of the finite effective all-partons-in-the-final-state matrix elements, in which partons a and b have simply been crossed to the initial state, i.e. in which their momenta $-p_a$ and -p_b have been replaced by p_a and p_b, as shown in the Fig. 1. The difference between $d\sigma_{ab}^{NLO}$ and $d\widehat{\sigma_{ab}^{NLO}}$ has been absorbed into the finite, universal crossing function $C_a^H(x,\mu_F)$. Defining a "effective" NLO parton distribution function $\mathcal{F}_a^H(x)$ as

$$\mathcal{F}_a^H(x) = f_a^H(x,\mu_F) + \alpha_s(\mu_R) C_a^H(x,\mu_F) + O(\alpha_s^2), \tag{7}$$

we can rewrite Eq. (6) in a simple form as

$$d\sigma_{H_1H_2}^{NLO} = \sum_{a,b} \int dx_1 dx_2 \mathcal{F}_a^{H_1}(x_1) \mathcal{F}_b^{H_2}(x_2) d\sigma_{ab}^{NLO}(x_1,x_2). \tag{8}$$

III. TREE LEVEL MATRIX ELEMENTS

The matrix elements of the scattering process $gb \to tW$ can be written in terms of the following twenty standard matrix elements that contain the information about the Dirac matrix structure:

$$\mathcal{M}_{LO} = \mathcal{M}_{LO}^{(s)} + \mathcal{M}_{LO}^{(t)}, \tag{9}$$

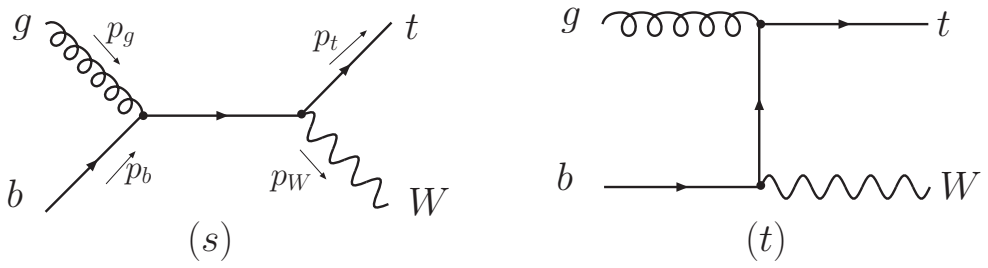

FIG. 2: Tree-level Feynman diagram of the $gb \to tW$ process.

where

$$\mathcal{M}_{LO}^{(i)} = -i\frac{g_s g}{\sqrt{2}} T_{ij}^a \epsilon^\mu(g) \varepsilon^{\nu *}(W)\, \bar{u}_t \Big[f_1^i g_{\mu\nu} + f_2^i \gamma_\mu \gamma_\nu + f_3^i p_{b,\nu}\gamma_\mu + f_4^i p_{b,\mu}\gamma_\nu + f_5^i p_{t,\nu}\gamma_\mu + f_6^i p_{t,\mu}\gamma_\nu + f_7^i p_{b,\mu}p_{b,\nu} + f_8^i p_{b,\mu}p_{t,\nu} + f_9^i p_{t,\mu}p_{b,\nu} + f_{10}^i p_{t,\mu}p_{t,\nu} + \not{p}_W (f_{11}^i g_{\mu\nu} + f_{12}^i \gamma_\mu\gamma_\nu + f_{13}^i p_{b,\nu}\gamma_\mu + f_{14}^i p_{b,\mu}\gamma_\nu + f_{15}^i p_{t,\nu}\gamma_\mu + f_{16}^i p_{t,\mu}\gamma_\nu + f_{17}^i p_{b,\mu}p_{b,\nu} + f_{18}^i p_{b,\mu}p_{t,\nu} + f_{19}^i p_{t,\mu}p_{b,\nu} + f_{20}^i p_{t,\mu}p_{t,\nu}) \Big] P_L u_b, \quad (10)$$

where $i = s(t)$. Here, $g_s(g)$ denotes the coupling strength of the strong (weak) interaction, respectively, $T_{i,j}^a$ are the color matrices in the fundamental representation, and $p_L \equiv (1 - \gamma_5)/2$ denotes the left-handed projector. The tree-level Feynman diagrams of the $gb \to tW$ process are shown in Fig. 2. The non-zero form factors of the tree-level matrix elements are given by

$$-f_3^s = f_4^s = f_5^s = f_{11}^s = 2f_{12}^s = \frac{2}{s}, \quad (11)$$

$$f_6^t = 2f_{12}^t = \frac{2}{t_1}. \quad (12)$$

The kinematics variables used in this paper are defined as follows:

$$s = (p_g + p_b)^2 = 2p_g \cdot p_b, \quad (13)$$

$$t = (p_g - p_t)^2 = t_1 + m_t^2, \quad (14)$$

$$u = (p_g - p_W)^2 = u_1 + m_W^2, \quad (15)$$

where $t_1 \equiv -2p_g \cdot p_t$, $u_1 \equiv -2p_g \cdot p_W$, and $s + t_1 + u_1 = 0$.

IV. VIRTUAL CORRECTIONS AND RENORMALIZATION

Now let us calculate the virtual corrections to the tW associated production. Fig. 3 shows the Feynman diagrams of the one-loop QCD virtual corrections, where V_i denote the

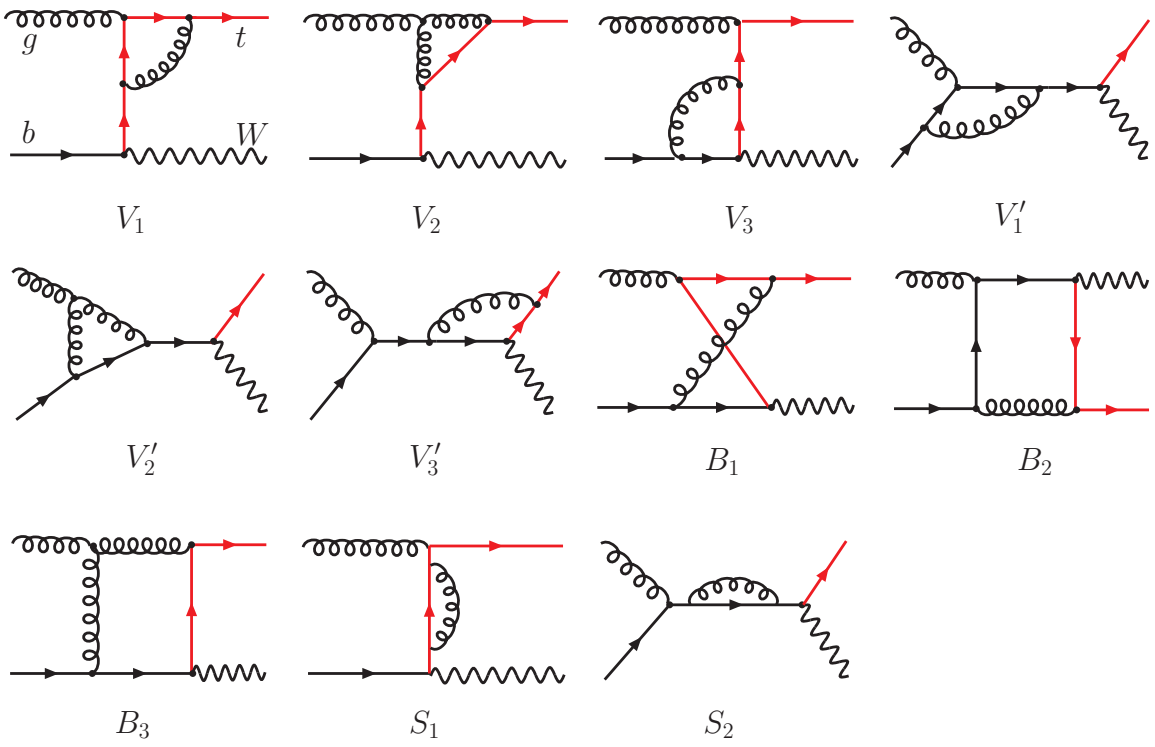

FIG. 3: Feynman diagrams of the one-loop virtual corrections where the red lines denote the top quark.

triangle loop corrections, B_i the box loop corrections, while S_i the bubble loop corrections. In this work we adapt the on-shell renormalization scheme such that the external self-energy corrections are cancelled by a set of counterterms which will be discussed later in this sections.

At the NLO the relevant one-loop virtual corrections contribute only through their interference with the lowest-order Born amplitudes. The interference, i.e. $\Re\left(\mathcal{M}_0\mathcal{M}^\dagger_{Virtual}\right)$, gives rise to the order of α_s^2 contributions. One can further categorize the virtual corrections into three classes, according to their color structures depicted in Fig. 4: (a) V_1, V_1', B_1, B_2; (b) V_3, V_3', S_1, S_2; (c) V_2, V_2', B_3. The color factors (CF) of those three classes, normalized to the Born level matrix element square, are given by

$$CF_a = -\frac{1}{2N_C}, \quad CF_b = \frac{N_C}{2} - \frac{1}{2N_C}, \quad CF_c = \frac{N_C}{2}. \tag{16}$$

The same color structures also apply to the real radiation corrections. Below we will make use of the color order to organize our calculation.

To calculate the virtual corrections, we follow the Passarino-Veltman procedure [52, 53]:

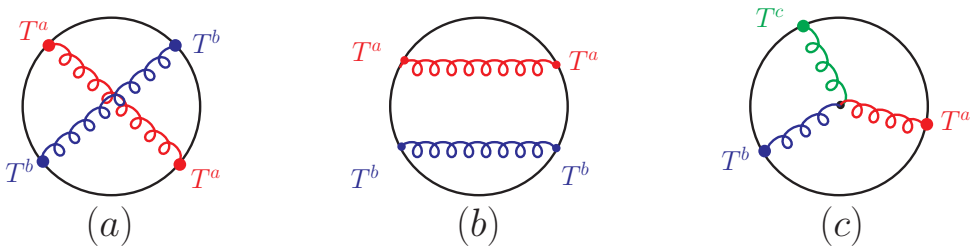

FIG. 4: Color factor of the interference of tree-level and one-loop matrix element.

one can reduce any set of vectorial of tensorial one-loop integrals to a few scalar functions. However, since the loop corrections exhibit not only the UV divergence but also the IR divergence, either soft or collinear or both, one needs to work out those scalar function analytically. Recently, a basis set of infra-red and/or collinearly divergent scalar oneloop integrals is constructed, and analytic formulas, for tadpole, bubble, triangle and box integrals, are given explicitly in Ref. [54]. The scalar functions used in this work can be found in that paper and those results are confirmed by our hand calculation. Our final results of the virtual corrections are very complicated, but the divergent pieces can be factorized out in a simple form. We present the full expressions and the divergent poles of the form factors in the Appendix C and D, respectively. We further distinguish between the UV and IR divergences in order to keep track on the renormalization and factorization.

Consider now the UV divergence first. We define $\Delta_{UV}(\mathcal{M}_i)$ to be the UV pole part of the corresponding amplitude $\mathcal{M}_i$. Using this notation, we find

$$\Delta_{UV}\left(\mathcal{M}_{V_1}+\mathcal{M}_{V_1'}\right) = \frac{\alpha_s}{4\pi}C_\epsilon\left(-\frac{1}{2N_C}\right)\frac{1}{\epsilon_{UV}}\mathcal{M}_{LO}, \tag{17}$$

$$\Delta_{UV}\left(\mathcal{M}_{V_2}+\mathcal{M}_{V_2'}\right) = \frac{\alpha_s}{4\pi}C_\epsilon\left(\frac{N_C}{2}\right)\frac{3}{\epsilon_{UV}}\mathcal{M}_{LO}, \tag{18}$$

$$\Delta_{UV}\left(\mathcal{M}_{V_3}+\mathcal{M}_{V_3'}\right) = \frac{\alpha_s}{4\pi}C_\epsilon\left(\frac{N_C}{2}-\frac{1}{2N_C}\right)\frac{1}{\epsilon_{UV}}\mathcal{M}_{LO}, \tag{19}$$

$$\Delta_{UV}\left(\mathcal{M}_{S_1}+\mathcal{M}_{S_2}\right) = \frac{\alpha_s}{4\pi}C_\epsilon\left(\frac{N_C}{2}-\frac{1}{2N_C}\right)\frac{-1}{\epsilon_{UV}}\mathcal{M}_{LO}+\mathcal{A}_{S_1}, \tag{20}$$

where $C_\epsilon \equiv (4\pi\mu^2/m_t^2)^2\Gamma\left(1+\epsilon\right)$. Note that $\mathcal{A}_{S_1}$ in Eq. 20 represents the non-factorization loop corrections originated from the Feynman diagram S_1, see Eqs. (C86-C88). The UV divergent poles of $\mathcal{A}_{S_1}$ are given in terms of the form factors as follows:

$$f_2^{\mathcal{A}_{S1}} = \frac{m_t}{t_1}\frac{3}{\epsilon_{UV}}, \qquad f_6^{\mathcal{A}_{S1}} = 2f_{12}^{\mathcal{A}_{S1}} = \frac{1}{\epsilon_{UV}}\left(\frac{12m_t^2}{t_1^2}-\frac{2}{t_1}\right). \tag{21}$$

As to be shown later, these non-factorisable divergences will be exactly cancelled by the top quark mass renormalization.

The renormalization is preformed in the $\overline{\rm MS}$ scheme with the top quark mass defined on shell. As required by renormalization group arguments, the renormalization of the fundamental propagators and interaction vertices of the theory reduces to introducing counterterms for the external field wave functions of top quarks and gluons (δZ_t, δZ_G), for the top mass (δm_t), and for the strong coupling constant (δg_s). We renormalize the fields of the gluons, $G_{a,\mu}$, of the bottom quark, ψ_b, and of the top quark, ψ_t, all in the on-shell scheme, i.e. the wave-function renormalization constants $\delta Z_{G,b,t}$, defined by the transformations

$$G^0_{a,\mu,} = \left(1+\frac{1}{2}\delta Z_G\right) G_{a,\mu}, \quad \psi^0_b = \left(1+\frac{1}{2}\delta Z_b\right)\psi_b, \quad \psi^0_t = \left(1+\frac{1}{2}Z_t\right)\psi_t, \tag{22}$$

are adjusted to cancel the external self-energy corrections exactly. Distinguishing between divergences of UV and IR origin, these constants can be written as

$$\delta Z_G = -\frac{\alpha_s}{4\pi}C_\epsilon\left\{\left(\frac{2}{3}n_f-\frac{5N_C}{3}\right)\left(\frac{1}{\epsilon_{UV}}-\frac{1}{\epsilon_{IR}}\right)-\frac{2}{3}\frac{1}{\epsilon_{UV}}\right\}, \tag{23}$$

$$\delta Z_t = -\frac{\alpha_s}{4\pi}C_\epsilon\left(\frac{N_C}{2}-\frac{1}{2N_C}\right)\left(\frac{1}{\epsilon_{UV}}+\frac{2}{\epsilon_{IR}}+4\right), \tag{24}$$

$$\delta Z_b = -\frac{\alpha_s}{4\pi}C_\epsilon\left(\frac{N_C}{2}-\frac{1}{2N_C}\right)\left(\frac{1}{\epsilon_{UV}}-\frac{1}{\epsilon_{IR}}\right), \tag{25}$$

where $n_f = 5$ is the number of light quark flavours.

Denoting the bare top quark mass and the bare strong coupling as m_t^0 and α_s^0, respectively, we introduce the renormalization parameters in the transformations

$$m_t^0 = m_t + \delta m_t, \qquad \alpha_s^0 = \alpha_s + \delta\alpha_s. \tag{26}$$

We defined the subtraction condition for the top quark mass m_t in such a way that m_t is the pole mass, in which case the top mass counterterm is given by

$$\frac{\delta m_t}{m_t} = -\frac{\alpha_s}{4\pi}C_\epsilon\left(\frac{N_C}{2}-\frac{1}{2N_C}\right)\left(\frac{3}{\epsilon_{UV}}+4\right). \tag{27}$$

Finally, for the renormalization of α_s, we use the $\overline{\rm MS}$ scheme, modified to decouple the top quark from the running of the strong coupling $\alpha_s(\mu)$. It gives rise to

$$\frac{\delta\alpha_s}{\alpha_s} = \frac{\alpha_s}{4\pi}\left\{(4\pi)^\epsilon\,\Gamma(1+\epsilon)\left(\frac{2n_f}{3}-\frac{11N_C}{3}\right)\frac{1}{\epsilon_{UV}}+\frac{2}{3}C_\epsilon\frac{1}{\epsilon_{UV}}\right\},$$

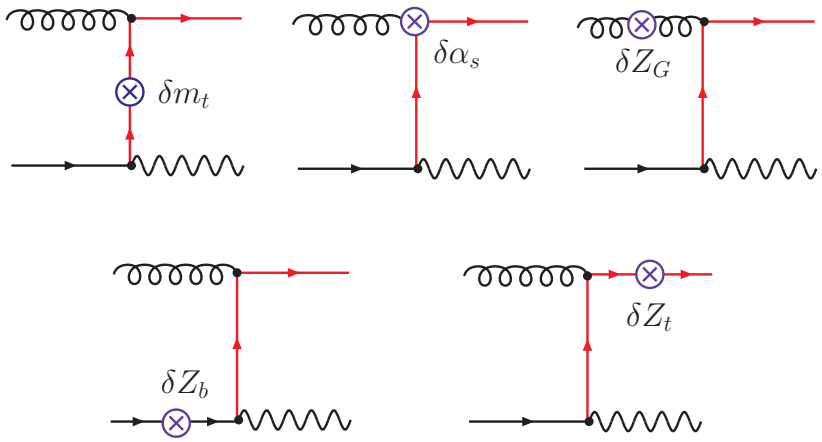

FIG. 5: Depicted Feynman diagrams of the counterterm contributions.

where the first term inside the braces originates from light quark and gluon loops, which is independent of μ, while the second term (proportional to C_ϵ) originates from the top quark loop in the gluon self-energy that is subtracted at zero-momentum transfer. In such a way the running of the coupling $\alpha_s(\mu)$ is generated solely by the finite contributions of the light quark and gluon loops, while the top quark contribution is absorbed completely in the renormalization condition and thus decouple effectively.

The contributions of the counterterms and the external self-energy to the one-loop matrix element are depicted in Fig. 5. The matrix elements is given by

$$\left(\frac{\delta\alpha_s}{\alpha_s}+\frac{1}{2}\delta Z_b+\frac{1}{2}\delta Z_t+\frac{1}{2}\delta Z_G\right)\mathcal{M}_{LO}+\mathcal{M}(\delta m_t). \tag{28}$$

The first term accounts for the external self-energy corrections as well as the counterterms of the strong coupling renormalization, while the second term proportional to δm_t comes from the renormalization of the top quark mass. After insertion of the top quark mass counterterm, see Fig. 5, we obtain the form factor of $\mathcal{M}(\delta m_t)$ as follows (where the color factor $\frac{N}{2}-\frac{1}{2N}$ is not shown explicitly):

$$f_2^{\delta m_t} = -\frac{m_t}{t_1}\left[\frac{3}{\epsilon_{UV}}+4\right], \tag{29}$$

$$f_6^{\delta m_t} = -\frac{m_t^2}{t_1^2}\left[\frac{12}{\epsilon_{UV}}+16\right], \tag{30}$$

$$f_{12}^{\delta m_t} = \frac{1}{2}f_6^{\delta m_t}. \tag{31}$$

In order to check the renormalization, we will combine $\mathcal{M}(\delta m_t)$ with those bubble, triangle and box loop corrections, therefore the renormalized matrix elements are given

by

$$\mathcal{M}_{ren} = \mathcal{M}_{virt} + \mathcal{M}_{CT}, \tag{32}$$

$$\mathcal{M}_{virt} = \left[\sum_{i=1}^{2}\mathcal{M}_{S_i} + \sum_{i=1}^{3}\left(\mathcal{M}_{V_i} + \mathcal{M}_{V_i'} + \mathcal{M}_{B_i}\right) + \mathcal{M}\left(\delta m_t\right)\right], \tag{33}$$

$$\mathcal{M}_{CT} = \left(\frac{\delta\alpha_s}{\alpha_s} + \frac{1}{2}\delta Z_b + \frac{1}{2}\delta Z_t + \frac{1}{2}\delta Z_G\right)\mathcal{M}_{LO}. \tag{34}$$

It is straightforward to check the UV divergences indeed cancel out, but the IR (soft and collinear) divergences still remain to be cancelled by the real radiation corrections. The IR poles of the virtual corrections are given by

$$\Delta_{IR}^{virt} = \mathcal{M}_{LO} \times \frac{\alpha_s}{4\pi} C_\epsilon \Bigg\{ -\frac{13}{\epsilon_{IR}^2} + \frac{3}{\epsilon_{IR}} \ln\frac{-t_1}{m_t^2} + \frac{3}{\epsilon_{IR}} \ln\frac{s}{m_t^2} - \frac{1}{3\epsilon_{IR}} \ln\frac{m_t^2 - m_W^2 - u}{m_t^2} - \frac{10}{3\epsilon_{IR}} - \frac{1}{2\epsilon_{IR}}\left(\frac{11N_C}{3} - \frac{2}{3}n_f\right)\Bigg\}. \tag{35}$$

V. INFRA-RED SINGULARITIES IN THE REAL EMISSION CORRECTIONS

In the one cutoff phase space slicing method, the theoretical cutoff parameter (s_{min}) is introduced in order to isolate soft and collinear singularities associated with real gluon emission sub-processes by partitioning the phase space into soft, collinear and hard regions such that

$$|\mathcal{M}^{\rm r}|^2 = |\mathcal{M}^{\rm r}|^2_{\rm soft} + |\mathcal{M}^{\rm r}|^2_{\rm collinear} + |\mathcal{M}^{\rm r}|^2_{\rm hard}\ . \tag{36}$$

In the soft and collinear regions the cross section is proportional to the Born-level cross section. Using dimensional regularization, we can evaluate the real gluon emission diagrams in n-dimensions under the soft gluon approximation in the soft region, or the collinear approximation in the collinear region, and can integrate out the corresponding phase space volume analytically. The resulting divergences are cancelled by virtual corrections or absorbed into the perturbative parton distribution functions in the factorization procedure.

In this method, a pair of partons with momenta p_i and p_j is defined to be unresolved if

$$|2p_i \cdot p_j| < s_{min}, \tag{37}$$

with s_{min} small compared to the hard scale of the process. This condition can occur if either p_i and p_j are collinear, or if one of the two is soft. When the scattering amplitude involves a complicated color structure, one needs to decompose the scattering amplitude

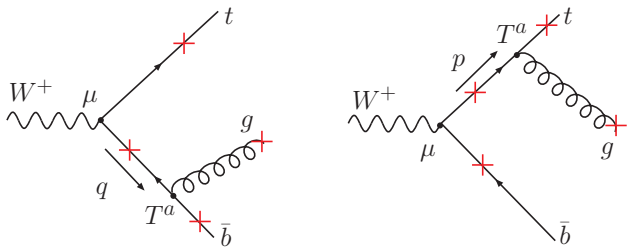

FIG. 6: Feynman diagrams of process $W' \to t\bar{b}g$ at Born level.

into color-ordered sub-amplitudes. Below we will use the tW associated production process to illustrate this point.

To calculate the real emission corrections, we first cross all the initial state partons to the final state and the final state W boson into the initial state, i.e. at the tree level,

$$gb \to W^- t \xrightarrow{crossing} W^+ \to t\bar{b}g.$$

The tree-level Feynman diagrams after crossing are shown in Fig. 6, which give rise to the following matrix element

$$\mathcal{M}_0 = -i\frac{g}{\sqrt{2}} g_s T^a \epsilon^\mu(W)\epsilon^{\sigma *}(g)\bar{u}(t)\left[\gamma^\sigma \frac{\not{p} + m_t}{p^2 - m_t^2}\gamma^\mu P_L + \gamma^\mu P_L \frac{-\not{q} + m_b}{q^2 - m_b^2}\gamma^\sigma\right] v(\bar{b}), \qquad (38)$$

where $q = p_g + p_{\bar{b}}$ and $p = p_t + p_g$. The cross symbol "$\times$" in the figure indicates the possible places where the additional parton can be radiated from. There are two types of real radiation corrections:

$$(1)\, W^+ \to t\bar{b}gg; \qquad (2)\, W^+ \to t\bar{b}q\bar{q}.$$

The former exhibits both soft and collinear divergences, but the latter can only have the collinear divergence.

A. Color ordered amplitude

For a systematic extraction of the infrared singularities within the one cutoff method, we organize the amplitude in terms of color-ordered sub-amplitudes. In Fig. 7, we present all the real emission diagrams which give rise to the final state of $t\bar{b}gg$. The color coefficients

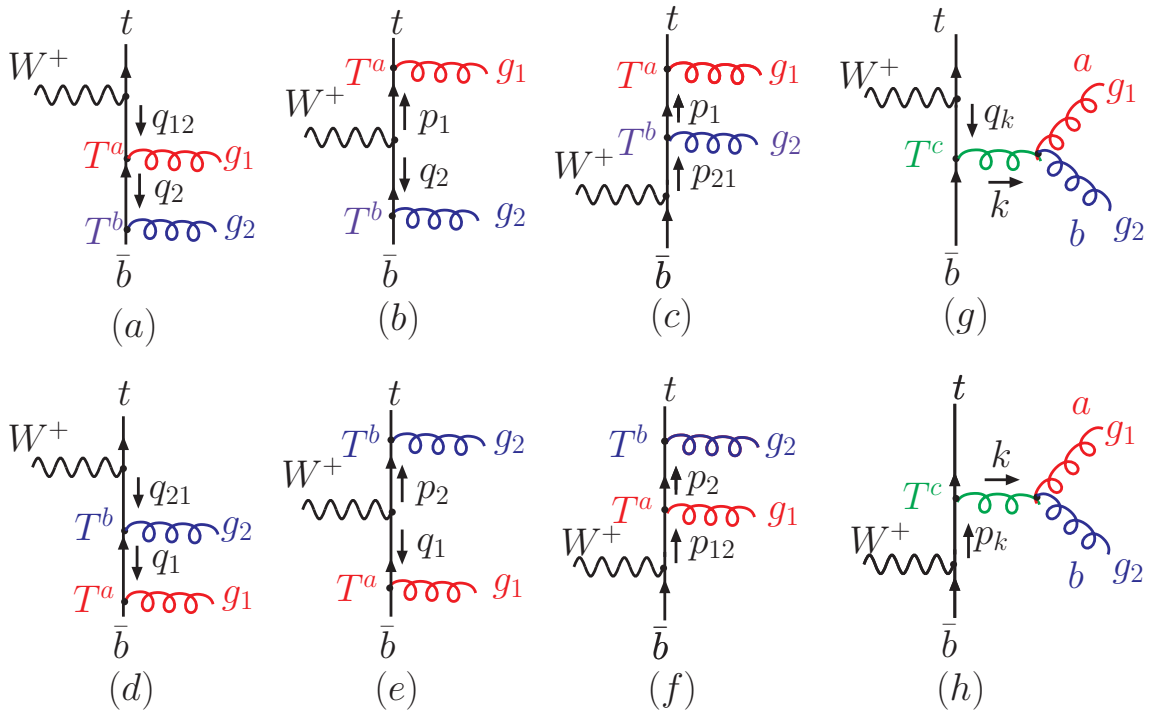

FIG. 7: Feynman diagrams contributing to $t\bar{b}gg$ final state.

of the diagrams are given as follows:

$$\begin{aligned} a, b, c &\propto T^a T^b, \\ d, e, f &\propto T^b T^a, \\ g, h &\propto T^a T^b \text{ and } T^b T^a, \end{aligned}$$

where we have applied the identity

$$if^{abc}T^c = T^a T^b - T^b T^c, \tag{39}$$

in the diagrams (g) and (h). Thus, we can decompose the amplitude $\mathcal{M}(W^+ \to t\bar{b}gg)$ as following,

$$\mathcal{M}(W^+ \to t\bar{b}gg) = T^a T^b \mathcal{M}_1 + T^b T^a \mathcal{M}_2, \tag{40}$$

where

$$\begin{aligned} \mathcal{M}_1 &= \mathcal{M}^{(a)} + \mathcal{M}^{(b)} + \mathcal{M}^{(c)} - \mathcal{M}^{(g)} - \mathcal{M}^{(h)}, \\ \mathcal{M}_2 &= \mathcal{M}^{(d)} + \mathcal{M}^{(e)} + \mathcal{M}^{(f)} + \mathcal{M}^{(g)} + \mathcal{M}^{(h)}. \end{aligned}$$

The color indices are assigned as shown in Fig. 7. The momentum q_i, q_{ij}, p_i and p_{ij} are defined as

$$p_i = p_t + p_{g_i}, \quad p_{ji} = p_t + p_{g_i} + p_{g_j},$$
$$q_i = p_b + p_{g_i}, \quad q_{ji} = p_b + p_{g_i} + p_{g_j}.$$

The amplitudes of diagrams (a, b, c) are given as follows (with a color coefficient $T^a T^b$):

$$\begin{aligned}
\mathcal{M}^{(a)} &= i\frac{g}{\sqrt{2}} g_s^2 \epsilon^\mu(W^+)\epsilon^{\rho*}(g_1)\epsilon^{\sigma*}(g_2) \\
&\times \bar{u}(t)\left[\gamma_\mu P_L \frac{-\not{q}_{12}+m_b}{q_{12}^2-m_b^2}\gamma_\rho \frac{-\not{q}_2+m_b}{q_2^2-m_b^2}\gamma_\sigma\right] v\left(\bar{b}\right), \qquad (41)\\
\mathcal{M}^{(b)} &= i\frac{g}{\sqrt{2}} g_s^2 \epsilon^\mu(W^+)\epsilon^{\rho*}(g_1)\epsilon^{\sigma*}(g_2) \\
&\times \bar{u}(t)\left[\gamma_\rho \frac{\not{p}_1+m_t}{p_1^2-m_t^2}\gamma_\mu P_L \frac{-\not{q}_2+m_b}{q_2^2-m_b^2}\gamma_\sigma\right] v\left(\bar{b}\right), \qquad (42)\\
\mathcal{M}^{(c)} &= i\frac{g}{\sqrt{2}} g_s^2 \epsilon^\mu(W^+)\epsilon^{\rho*}(g_1)\epsilon^{\sigma*}(g_2) \\
&\times \bar{u}(t)\left[\gamma_\rho \frac{\not{p}_1+m_t}{p_1^2-m_t^2}\gamma_\sigma \frac{\not{p}_{21}+m_t}{p_{21}^2-m_t^2}\gamma_\mu P_L\right] v\left(\bar{b}\right). \qquad (43)
\end{aligned}$$

The amplitudes of diagrams (d, e, f) are given as follows (with a color coefficient $T^b T^a$):

$$\begin{aligned}
\mathcal{M}^{(d)} &= i\frac{g}{\sqrt{2}} g_s^2 \epsilon^\mu(W^+)\epsilon^{\rho*}(g_1)\epsilon^{\sigma*}(g_2) \\
&\times \bar{u}(t)\left[\gamma_\mu P_L \frac{-\not{q}_{21}+m_b}{q_{21}^2-m_b^2}\gamma_\sigma \frac{-\not{q}_1+m_b}{q_1^2-m_b^2}\gamma_\rho\right] v\left(\bar{b}\right), \qquad (44)\\
\mathcal{M}^{(e)} &= i\frac{g}{\sqrt{2}} g_s^2 \epsilon^\mu(W^+)\epsilon^{\rho*}(g_1)\epsilon^{\sigma*}(g_2) \\
&\times \bar{u}(t)\left[\gamma_\sigma \frac{\not{p}_2+m_t}{p_2^2-m_t^2}\gamma_\mu P_L \frac{-\not{q}_1+m_b}{q_1^2-m_b^2}\gamma_\rho\right] v\left(\bar{b}\right), \qquad (45)\\
\mathcal{M}^{(f)} &= i\frac{g}{\sqrt{2}} g_s^2 \epsilon^\mu(W^+)\epsilon^{\rho*}(g_1)\epsilon^{\sigma*}(g_2) \\
&\times \bar{u}(t)\left[\gamma_\sigma \frac{\not{p}_2+m_t}{p_2^2-m_t^2}\gamma_\rho \frac{\not{p}_{12}+m_t}{p_{12}^2-m_t^2}\gamma_\mu P_L\right] v\left(\bar{b}\right). \qquad (46)
\end{aligned}$$

Finally, the amplitudes of diagrams (g, h) are given as follows (with a color coefficient $-if^{abc}T^c$):

$$\begin{aligned}
\mathcal{M}^{(g)} &= i\frac{g}{\sqrt{2}} g_s^2 \epsilon^\mu(W^+)\epsilon^{\rho*}(g_1)\epsilon^{\sigma*}(g_2) \\
&\times \bar{u}(t)\left[\gamma_\mu P_L \frac{-\not{q}_k+m_b}{q_k^2-m_b^2}\gamma_\alpha\right] v\left(\bar{b}\right) \frac{1}{k^2} V^{\rho\sigma\alpha}, \qquad (47)
\end{aligned}$$

$$\mathcal{M}^{(h)} = i\frac{g}{\sqrt{2}}g_s^2\epsilon^{\mu}(W^+)\epsilon^{\rho *}(g_1)\epsilon^{\sigma *}(g_2)$$
$$\times\ \bar{u}(t)\left[\gamma_\alpha\frac{\not{p}_k + m_t}{p_k^2 - m_t^2}\gamma_\mu P_L\right]v\left(\bar{b}\right)\frac{1}{k^2}V^{\rho\sigma\alpha}, \tag{48}$$

where

$$V^{\rho\sigma\alpha} = g^{\rho\sigma}\left(p_{g_1} - p_{g_2}\right)^{\alpha} + g^{\sigma\alpha}\left(k + p_{g_2}\right)^{\rho} - g^{\alpha\rho}\left(k + p_{g_1}\right)^{\sigma}. \tag{49}$$

The squared amplitude, after summing over colors and spins, are given by

$$\sum_{\substack{\text{color}\\ \text{spin}}}\left|\mathcal{M}(W^+ \to t\bar{b}gg)\right|^2$$
$$= \frac{N_C^2 - 1}{2}\frac{N_C}{2}\left[\left|\mathcal{M}_1\right|^2 + \left|\mathcal{M}_2\right|^2 - \frac{1}{N_C^2}\left|\mathcal{M}_1 + \mathcal{M}_2\right|^2\right], \tag{50}$$

where summing over the final state degrees of freedom is understood in $|\mathcal{M}_i|^2$. The factorization of soft and collinear singularities for color ordered amplitudes has been discussed in the literature mainly for the leading color terms ($\mathcal{O}(N)$) [41, 42]. For our calculation of the one cutoff phase space slicing method, we will have to extend these results to the sub-leading color terms ($\mathcal{O}(1/N)$).

B. Soft singularities

The soft gluon behavior for an color ordered sub-amplitude is very similar to the soft photon behavior of QED amplitudes. In QED, the soft photon couples to a charged fermion line, resulting in an eikonal factor multiplying the hard process. The key point is that only the Feynman diagrams with soft photon coupled to the external charged fermion lines will contribute in the soft photon limit. Technically, no matter how many photons are radiated out from the charged fermion dipole, the soft eikonal factor only knows about the external momentum since there is no photon-photon interaction in QED theory. In QCD, the soft pattern becomes much complicated due to the non-Abelian interaction. However, it has been shown that the color ordered sub-amplitudes do exhibit a factorization of the soft gluon singularities as in the QED [55, 56]. This is because the partons are ordered and form well defined color charge lines to which the soft gluon can couple. The soft gluon behavior depends only on the momenta of the external color charged lines to which the soft gluon couples, and is independent of the number and type of other partons in the process.

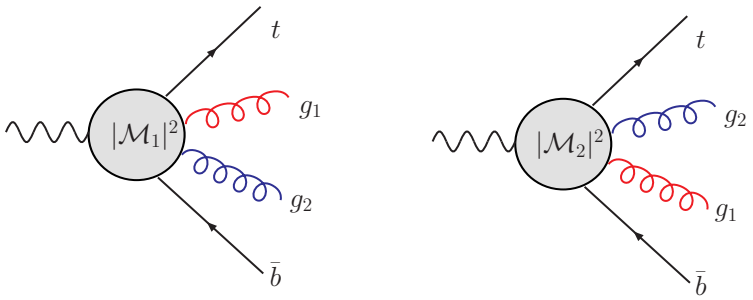

FIG. 8: Momentum label of the color ordered amplitudes.

Similarly, the soft factor is independent of whether or not any color singlet particles such as electroweak bosons are participating in the hard process.

1. *Factorization of the color ordered amplitudes in the soft limit*

In the limit of one gluon being soft, each term in the squared amplitudes (cf. Eq. 50) can be written as a factor multiplying the Born level amplitude square. Since t and $\bar{b}$ are the external fermions which cannot be soft, there are only two sources of the soft singularities: either from g_1 or from g_2. When both of them are soft, it goes beyond the NLO ($\mathcal{O}(\alpha_s^2)$) and will not be considered in our calculation.

First consider $|\mathcal{M}_{1,2}|^2$. The momentum configurations which respect the color order are shown in Fig. 8. In the soft gluon limit, $|\mathcal{M}_1|^2$ can be factorized as follows:

$$\frac{N_C^2-1}{2}\frac{N_C}{2}\left|\mathcal{M}_1\right|^2 \xrightarrow{g_1\to 0} \frac{g_s^2 N_C}{2} f\left(t,g_1,g_2\right)\left|\mathcal{M}_0\right|^2, \tag{51}$$

$$\xrightarrow{g_2\to 0} \frac{g_s^2 N_C}{2} f(g_1,g_2,\bar{b})\left|\mathcal{M}_0\right|^2, \tag{52}$$

where the eikonal factor $f(a,s,b)$ is defined as

$$f\left(a,s,b\right)=\frac{4s_{ab}}{s_{as}s_{sb}}-\frac{4m_a^2}{s_{as}^2}-\frac{4m_b^2}{s_{sb}^2}. \tag{53}$$

Here we define $s_{ij}=2p_i\cdot p_j$ for both massive and massless partons. The color factor $(N_C^2-1)/2$ has been absorbed into the Born level amplitude square. Similarly, $|\mathcal{M}_2|^2$ can be factorized in the soft gluon limit as follows:

$$\frac{N_C^2-1}{2}\frac{N_C}{2}\left|\mathcal{M}_2\right|^2 \xrightarrow{g_1\to 0} \frac{g_s^2 N_C}{2} f\left(g_2,g_1,\bar{b}\right)\left|\mathcal{M}_0\right|^2, \tag{54}$$

$$\xrightarrow{g_2\to 0} \frac{g_s^2 N_C}{2} f(t,g_2,g_1)\left|\mathcal{M}_0\right|^2. \tag{55}$$

Now let us consider the QED-like term $|\mathcal{M}_1+\mathcal{M}_2|^2$. This interference term exhibits the canonical eikonal factorization in the soft limit. The soft gluon only knows about the external color charged fermion lines, leading to the following factorization

$$-\frac{N_C^2-1}{2}\frac{1}{2N_C}\left|\mathcal{M}_1+\mathcal{M}_2\right|^2 \xrightarrow{g_1\to 0} -\frac{g_s^2}{2N_C}\,f\left(t,g_1,\bar{b}\right)\left|\mathcal{M}_0\right|^2, \tag{56}$$

$$\xrightarrow{g_2\to 0} -\frac{g_s^2}{2N_C}\,f(t,g_2,\bar{b})\left|\mathcal{M}_0\right|^2. \tag{57}$$

2. soft singularities of $|\mathcal{M}_1|^2$

In order to slice the phase space we introduce the following Heaviside functions $\Theta(i,j,k)$ and $\bar{\Theta}(i,j,k)$:

$$\Theta(i,j,k) \equiv \Theta(s_{ij}+s_{jk}-2s_{min}), \tag{58}$$

$$\bar{\Theta}(i,j,k) \equiv \Theta(2s_{min}-s_{ij}-s_{jk}). \tag{59}$$

With the help of Θ-functions we can split the phase space of the real emission corrections into four regions:

$$\begin{aligned} 1 &= \left(\Theta_{tg_1g_2}+\bar{\Theta}_{tg_1g_2}\right)\left(\Theta_{g_1g_2\bar{b}}+\bar{\Theta}_{g_1g_2\bar{b}}\right) \\ &= \Theta_{tg_1g_2}\Theta_{g_1g_2\bar{b}}+\Theta_{tg_1g_2}\bar{\Theta}_{g_1g_2\bar{b}}+\bar{\Theta}_{tg_1g_2}\Theta_{g_1g_2\bar{b}}-\bar{\Theta}_{tg_1g_2}\bar{\Theta}_{g_1g_2\bar{b}}. \end{aligned} \tag{60}$$

The first term denotes the region where two gluons are both hard (no soft singularities), but one should keep in mind that there might exist the collinear divergences, depending on the masses of external fermions. The second term denotes the region where the gluon g_2 is soft but the gluon g_1 is hard. The third term denotes the region where g_1 is soft and g_2 is hard. The last term denotes the region where g_1 and g_2 are both soft. As discussed before, this region only contributes when one calculates the quantum corrections beyond the next-to-leading order and therefore is ignored in this work. The negative sign ahead of the fourth term is to get rid of the double counting from the regions described in the second and third terms.

When g_1 is soft, the eikonal factor $f(t,g_1,g_2)$,

$$f(t,g_1,g_2) = \frac{4s_{tg_2}}{s_{tg_1}s_{g_1g_2}}-\frac{4m_t^2}{s_{tg_1}^2}, \tag{61}$$

can be calculated in the center frame of (t, g_2) system where we choose the explicit momentum of final state particles as follows:

$$\begin{aligned} p_t &= (E_t, 0, 0, \beta_t E_t)\,, \\ p_{g_2} &= (\beta_t E_t, 0, 0, -\beta_t E_t)\,, \\ p_{g_1} &= (E_{g_1}, 0, E_{g_1}\sin\theta, E_{g_1}\cos\theta)\,. \end{aligned}$$

Here, E_t, E_{g_1} and E_{g_2} is the energy of the top quark, the soft gluon (g_1) and the hard gluon (g_2), respectively, and θ is the angle between the soft gluon g_1 and the top quark. It is easy to show that the eikonal factor can be written as

$$f(t, g_1, g_2) = \frac{1}{E_{g_1}^2 E_t}\left(\frac{2\sqrt{s_{tg_2}+m_t^2}}{(1+\cos\theta)(1-\beta_t\cos\theta)} - \frac{m_t^2}{E_t(1-\beta_t\cos\theta)^2}\right), \tag{62}$$

where

$$\begin{aligned} s_{tg_2} &= 2\beta E_t^2(1+\beta), \\ \beta_t &= \frac{s_{tg_2}}{s_{tg_2}+2m^2}, \\ E_t &= \frac{s_{tg_2}+2m_t^2}{2\sqrt{s_{tg_2}+m_t^2}}. \end{aligned}$$

Now let us calculate the phase space boundary condition with the choice of momentum above. The sum of s_{tg_1} and $s_{g_1g_2}$ is given by

$$s_{tg_1} + s_{g_1g_2} = 2E_tE_{g_1}(1+\beta_t) = 2E_{g_1}\sqrt{s_{tg_2}+m_t^2}. \tag{63}$$

Substituting Eq. 63 into the soft phase space boundary condition, we obtain the upper limit of E_{g_1},

$$E_{g_1} \le \frac{s_{min}}{\sqrt{s_{tg_2}+m_t^2}} \equiv E_{g_1}^{max}.$$

In the soft limit, the phase space is also factorizes as

$$d^n\Phi_4 \xrightarrow{p_{g_1}\to 0} d^n\Phi_3 \frac{1}{8\pi^2}\frac{(4\pi)^\epsilon}{\Gamma(1-\epsilon)} E_{g_1}^{1-2\epsilon}\sin^{1-2\epsilon}\theta\, dE_{g_1} d\theta. \tag{64}$$

Then the soft gluon contribution is given by

$$\begin{aligned} & I^{soft}(t, g_1, g_2) \\ =& \int \bar{\Theta}_{tg_1g_2}\left[\frac{g_s^2 N_C}{2}\left(\mu_d^2\right)^\epsilon f(t, g_1, g_2)\frac{d^3g_1}{(2\pi)^{d-1}2E_{g_1}}\right] \\ =& N_C\frac{g_s^2}{2}\frac{1}{8\pi^2}\frac{(4\pi\mu_d^2)^\epsilon}{\Gamma(1-\epsilon)}\int_0^{E_{g_1}^{max}} E_{g_1}^{-1-2\epsilon}\mathrm{d}E_{g_1} \\ \times& \int_0^\pi \sin^{1-2\epsilon}\theta\frac{1}{E_t}\left[\frac{2\sqrt{s_{tg_2}+m_t^2}}{(1+\cos\theta)\,(1-\beta_t\cos\theta)} - \frac{m_t^2}{E_t\,(1-\beta_t\cos\theta)^2}\right]\mathrm{d}\theta. \end{aligned} \tag{65}$$

Using the formula listed in Appendix A we evaluate the integral in Eq. 65 and obtain the soft factor $I^{soft}(t, g_1, g_2)$ as following,

$$\begin{aligned} I^{soft}(t, g_1, g_2) &= N_C \frac{g_s^2}{16\pi^2} \frac{1}{\Gamma(1-\epsilon)} \left(\frac{4\pi\mu_d^2}{s_{min}}\right)^{\epsilon} \left(\frac{s_{min}}{s_{tg_2} + m_t^2}\right)^{-\epsilon} \\ &\times \left\{ \frac{1}{\epsilon_{IR}^2} - -\frac{1}{\epsilon_{IR}} \left[\ln\left(1 + \frac{s_{tg_2}}{m_t^2}\right) + 2\ln 2 - 1 \right] \right. \\ &\quad -\frac{\pi^2}{6} + 2\ln^2 2 - 2\ln 2 + \left[2\ln 2 + \frac{s_{tg_2} + 2m_t^2}{s_{tg_2}} \right] \ln\left(1 + \frac{s_{tg_2}}{m_t^2}\right) \\ &\quad \left. -\frac{1}{2}\ln^2\left(1 + \frac{s_{tg_2}}{m_t^2}\right) - 2\mathrm{Li}_2\left(\frac{s_{tg_2}}{s_{tg_2} + m_t^2}\right) \right\}. \end{aligned} \tag{66}$$

Similarly, one can calculate the soft singularity when g_2 is soft, yielding

$$\begin{aligned} I^{soft}(g_1, g_2, \bar{b}) &= \int \bar{\Theta}_{g_1 g_2 \bar{b}} \left[\frac{g_s^2 N_C}{2} \left(\mu_d^2\right)^{\epsilon} f(g_1, g_2, \bar{b}) \frac{d^3 g_2}{(2\pi)^{d-1} 2E_{g_2}} \right] \\ &= N_C \frac{g_s^2}{16\pi^2} \frac{1}{\Gamma(1-\epsilon)} \left(\frac{4\pi\mu_d^2}{s_{min}}\right) \left(\frac{s_{min}}{s_{g_1\bar{b}}}\right)^{-\epsilon} \\ &\times \left\{ \frac{2}{\epsilon_{IR}^2} - \frac{4\ln 2}{\epsilon_{IR}} + 4\ln^2 2 - \frac{\pi^2}{3} \right\}. \end{aligned} \tag{67}$$

This result is for $m_b = 0$ only. If $m_b \neq 0$, then the soft factor can be obtained from Eq. 66,

$$\begin{aligned} I^{soft}(g_1, g_2, \bar{b}) &= N_C \ \frac{g_s^2}{16\pi^2} \frac{1}{\Gamma(1-\epsilon)} \left(\frac{4\pi\mu_d^2}{s_{min}}\right)^{\epsilon} \left(\frac{s_{min}}{s_{g_1\bar{b}} + m_b^2}\right)^{-\epsilon} \\ &\times \quad \left\{ \frac{1}{\epsilon^2} - \frac{1}{\epsilon} \left[\ln\left(1 + \frac{s_{g_1\bar{b}}}{m_b^2}\right) + 2\ln 2 - 1 \right] \right. \\ &\quad -\frac{\pi^2}{6} + 2\ln^2 2 - 2\ln 2 + \left[2\ln 2 + \frac{s_{g_1\bar{b}} + 2m_b^2}{s_{g_1\bar{b}}} \right] \ln\left(1 + \frac{s_{g_1\bar{b}}}{m_b^2}\right) \\ &\quad \left. -\frac{1}{2}\ln^2\left(1 + \frac{s_{g_1\bar{b}}}{m_b^2}\right) - 2\mathrm{Li}_2\left(\frac{s_{g_1\bar{b}}}{s_{g_1\bar{b}} + m_b^2}\right) \right\}. \end{aligned} \tag{68}$$

3. soft singularities of $|\mathcal{M}_2|^2$

The phase space can be splitted into four regions:

$$\begin{aligned} 1 &= \left(\Theta_{tg_2g_1} + \bar{\Theta}_{tg_2g_1}\right)\left(\Theta_{g_2g_1\bar{b}} + \bar{\Theta}_{g_2g_1\bar{b}}\right) \\ &= \Theta_{tg_2g_1}\Theta_{g_2g_1\bar{b}} + \Theta_{tg_2g_1}\bar{\Theta}_{g_2g_1\bar{b}} + \bar{\Theta}_{tg_2g_1}\Theta_{g_2g_1\bar{b}} - \bar{\Theta}_{tg_2g_1}\bar{\Theta}_{g_2g_1\bar{b}}. \end{aligned} \tag{69}$$

The soft singularities of $|\mathcal{M}_2|^2$ can be derived from the results of $|\mathcal{M}_1|^2$ by making the substitution $g_1 \leftrightarrow g_2$.

4. soft singularities of $|\mathcal{M}_1+\mathcal{M}_2|^2$

The phase space can be splitted into

$$\begin{aligned} 1 &= \left(\Theta_{tg_1\bar{b}}+\bar{\Theta}_{tg_1\bar{b}}\right)\left(\Theta_{tg_2\bar{b}}+\bar{\Theta}_{tg_2\bar{b}}\right) \\ &= \Theta_{tg_1\bar{b}}\Theta_{tg_2\bar{b}}+\Theta_{tg_1\bar{b}}\bar{\Theta}_{tg_2\bar{b}}+\bar{\Theta}_{tg_1\bar{b}}\Theta_{tg_2\bar{b}}-\bar{\Theta}_{tg_1\bar{b}}\bar{\Theta}_{tg_2\bar{b}}. \end{aligned} \tag{70}$$

The first term corresponds to the two hard gluons, the second term denotes $E_{g_1}\to 0$, the third term denotes $E_{g_2}\to 0$ and the fourth term denotes both $E_{g_1}\to 0$ and $E_{g_2}\to 0$. Since the eikonal factor is only determined by the two external fermion lines (t and $\bar{b}$), the soft factors of g_1 and g_2 should be the same, i.e.

$$I^{soft}(t,g_1,\bar{b}) = I^{soft}(t,g_2,\bar{b}). \tag{71}$$

The soft factor can easily be derived from that of $\bar{\Theta}_{tg_1g_2}\left|\mathcal{M}_1\right|^2$ by making the substitution $g_2\to\bar{b}$, because the soft gluon contributions only know about the kinematics. It gives rise to the soft factor as following,

$$\begin{aligned} I^{soft}(t,g_1,\bar{b}) &= I^{soft}(t,g_1,g_2)\big|_{g_2\to\bar{b}} \\ &= \left(-\frac{1}{N_C}\right)\frac{g_s^2}{16\pi^2}\frac{1}{\Gamma(1-\epsilon)}\left(\frac{4\pi\mu_d^2}{s_{min}}\right)^{\epsilon}\left(\frac{s_{min}}{s_{t\bar{b}}+m_t^2}\right)^{-\epsilon} \\ &\times \left\{\frac{1}{\epsilon_{IR}^2}--\frac{1}{\epsilon_{IR}}\left[\ln\left(1+\frac{s_{t\bar{b}}}{m_t^2}\right)+2\ln 2-1\right]\right. \\ &\quad -\frac{\pi^2}{6}+2\ln^2 2-2\ln 2+\left[2\ln 2+\frac{s_{t\bar{b}}+2m_t^2}{s_{t\bar{b}}}\right]\ln\left(1+\frac{s_{t\bar{b}}}{m_t^2}\right) \\ &\quad \left.-\frac{1}{2}\ln^2\left(1+\frac{s_{t\bar{b}}}{m_t^2}\right)-2\mathrm{Li}_2\left(\frac{s_{t\bar{b}}}{s_{t\bar{b}}+m_t^2}\right)\right\}. \end{aligned} \tag{72}$$

C. Collinear singularities

As mentioned above, there still exists collinear divergence even for a hard gluon radiation. Below we will further slice the collinear region of the phase space to derive the collinear divergences.

1. Collinear singularities of $|\mathcal{M}|_1^2$

We further slice the hard phase space of $|\mathcal{M}|_1^2$ as

$$\Theta_{tg_1g_2}\Theta_{g_1g_2\bar{b}}\left|\mathcal{M}_1\right|^2 = \left\{\Theta_{tg_1g_2}\Theta_{g_1g_2\bar{b}}-C_{\mathcal{M}_1}+C_{\mathcal{M}_1}\right\}\left|\mathcal{M}_1\right|^2, \tag{73}$$

where

$$C_{\mathcal{M}_1} = \Theta\left(s_{tg_1} - 2s_{min}\right)\Theta\left(s_{g_2\bar{b}} - 2s_{min}\right)\Theta\left(s_{min} - s_{g_1g_2}\right) + \Theta\left(s_{t\bar{b}} - 2s_{min}\right)\Theta\left(s_{g_1g_2} - 2s_{min}\right)\Theta\left(s_{min} - s_{g_2\bar{b}}\right). \quad (74)$$

The first term in $C_{\mathcal{M}_1}$ represents the phase space region that neither g_1 or g_2 is not soft but $g_1 \parallel g_2$, while the second term denotes the phase space region of $g_2 \parallel \bar{b}$.

In the collinear region of $g_1 \parallel g_2$, the color ordered matrix element square exhibits the following factorization property,

$$\frac{N_C}{2}\frac{N_C^2-1}{2}\left|\mathcal{M}_1\right|^2 \xrightarrow{g_1\parallel g_2} \frac{g_s^2 N_C}{2} f^{gg\to g}\left|\mathcal{M}_0\right|^2, \quad (75)$$

where

$$f^{gg\to g}(\xi) = \frac{2}{s_{g_1g_2}}\frac{1+\xi^4+(1-\xi)^4}{\xi(1-\xi)} - \frac{4m_t^2}{\xi^2 s_{th}^2}, \quad (76)$$

with the kinematics defined as

$$p_h = p_{g_1} + p_{g_2}, \quad p_{g_1} = \xi p_h, \quad p_{g_2} = (1-\xi)\, p_h. \quad (77)$$

The phase space integration in the collinear region can also be written in the following factorization form

$$\frac{d^n p_{g_1}}{(2\pi)^{n-1}\, 2E_{g_1}}\frac{d^n p_{g_2}}{(2\pi)^{n-1}\, 2E_{g_2}} = \frac{1}{16\pi^2}\frac{(4\pi)^\epsilon}{\Gamma(1-\epsilon)}\left[s_{g_1g_2}\xi(1-\xi)\right]^{-\epsilon} ds_{g_1g_2} d\xi \times \frac{d^d p_h}{(2\pi)^{d-1}\, 2E_h}. \quad (78)$$

Bearing in mind that the integration is limited by the conditions $s_{g_1g_2} < s_{min}$, $s_{tg_1} > 2s_{min}$ and $s_{g_2\bar{b}} > 2s_{min}$, we integrate the matrix element over the collinear phase space and obtain the following collinear factor,

$$C_{\mathcal{M}_1}^{gg\to g} = \frac{\alpha_s}{4\pi}\frac{N_C}{\Gamma(1-\epsilon)}\left(\frac{4\pi\mu}{s_{min}}\right)^2\left\{\frac{2}{\epsilon_{IR}}\left[\ln\frac{2s_{min}}{s_{tg_1}} + \ln\frac{2s_{min}}{s_{g_1\bar{b}}} + \frac{11}{6}\right] - \frac{2m_t^2}{s_{tg_1}} - \frac{2\pi^2}{3} + \frac{67}{9} - \ln^2\frac{2s_{min}}{s_{tg_1}} - \ln^2\frac{2s_{min}}{s_{g_1\bar{b}}}\right\}. \quad (79)$$

In the collinear region of $g_2 \parallel \bar{b}$, the color ordered matrix element square exhibits the following factorization property,

$$\frac{N_C}{2}\frac{N_C^2-1}{2}\left|\mathcal{M}_1\right|^2 \xrightarrow{g_2\parallel\bar{b}} \frac{g_s^2 N_C}{2} f^{qg\to q}\left|\mathcal{M}_0\right|^2, \quad (80)$$

where

$$f^{qg\to q}(\xi)=\frac{2}{s_{g_2\bar{b}}}\frac{1+\xi^2-\epsilon(1-\xi)^2}{(1-\xi)}. \tag{81}$$

Again, after integrating over the collinear phase space, we obtain the following collinear factor,

$$C^{qg\to q}_{\mathcal{M}_1}=\frac{\alpha_s}{4\pi}\frac{N_C}{\Gamma(1-\epsilon)}\left(\frac{4\pi\mu}{s_{min}}\right)^2\left\{\frac{2}{\epsilon_{IR}}\left[\ln\frac{2s_{min}}{s_{g_1\bar{b}}}+\frac{3}{4}\right]-\frac{\pi^2}{3}+\frac{7}{2}-\ln^2\frac{2s_{min}}{s_{g_1\bar{b}}}\right\}. \tag{82}$$

2. Collinear singularities of $|\mathcal{M}_2|^2$

Similar to the case of $|\mathcal{M}_1|^2$, we split the hard phase space of $|\mathcal{M}_2|^2$ as

$$\Theta_{tg_2g_1}\Theta_{g_2g_1\bar{b}}|\mathcal{M}_2|^2=\left[\Theta_{tg_2g_1}\Theta_{g_2g_1\bar{b}}-C_{\mathcal{M}_2}+C_{\mathcal{M}_2}\right]|\mathcal{M}_2|^2, \tag{83}$$

where

$$\begin{aligned}C_{\mathcal{M}_2} &= \Theta(s_{tg_2}-2s_{min})\,\Theta\left(s_{g_1\bar{b}}-2s_{min}\right)\Theta(s_{min}-s_{g_2g_1})\\ &+ \Theta(s_{t\bar{b}}-2s_{min})\,\Theta(s_{g_2g_1}-2s_{min})\,\Theta\left(s_{min}-s_{g_1\bar{b}}\right).\end{aligned} \tag{84}$$

The first (second) term in $C_{\mathcal{M}_2}$ represents the collinear region of $g_2\parallel g_1$ ($g_1\parallel\bar{b}$), respectively. The collinear factors can be derived on the analogy of those of $|\mathcal{M}_1|^2$,

$$C^{gg\to g}_{\mathcal{M}_2}=C^{gg\to g}_{\mathcal{M}_1},\quad C^{qg\to q}_{\mathcal{M}_2}=C^{qg\to q}_{\mathcal{M}_2}. \tag{85}$$

3. Collinear singularities of $|\mathcal{M}_1+\mathcal{M}_2|^2$

We split the hard phase space of $|\mathcal{M}_1+\mathcal{M}_2|^2\equiv\mathcal{M}_{1+2}$ as

$$\Theta_{tg_1\bar{b}}\Theta_{tg_2\bar{b}}|\mathcal{M}_{1+2}|^2=\left[\Theta_{tg_1\bar{b}}\Theta_{tg_2\bar{b}}-C_{\mathcal{M}_{1+2}}+C_{\mathcal{M}_{1+2}}\right]|\mathcal{M}_{1+2}|^2, \tag{86}$$

where

$$\begin{aligned}C_{\mathcal{M}_{1+2}} &= \Theta(s_{tg_1}-2s_{min})\,\Theta\left(s_{g_2\bar{b}}-2s_{min}\right)\Theta\left(s_{min}-s_{g_1\bar{b}}\right)\\ &+ \Theta(s_{tg_2}-2s_{min})\,\Theta\left(s_{g_1\bar{b}}-2s_{min}\right)\Theta\left(s_{min}-s_{g_2\bar{b}}\right).\end{aligned} \tag{87}$$

The first (second) term in $C_{\mathcal{M}_{1+2}}$ represents the collinear region of $g_1\parallel\bar{b}$ ($g_2\parallel\bar{b}$), respectively. In both collinear regions, the matrix element square can be factorized as

$$-\frac{N_C^2-1}{2}\frac{1}{2N_C}|\mathcal{M}_{1+2}|^2\xrightarrow{g_i\parallel\bar{b}}-\frac{g_s^2}{2N_C}f^{qg_i\to q}|\mathcal{M}_0|^2. \tag{88}$$

Integration over the collinear region gives rise to the following collinear factor,

$$\begin{aligned} & C_{\mathcal{M}_{1+2}}^{qg_1\to q} = C_{\mathcal{M}_{1+2}}^{qg_2\to q} \\ = & -\frac{\alpha_s}{4\pi}\frac{1}{N_C}\frac{1}{\Gamma(1-\epsilon)}\left(\frac{4\pi\mu^2}{s_{min}}\right)^2\left\{\frac{2}{\epsilon_{IR}}\left[\ln\frac{2s_{min}}{s_{t\bar{b}}}+\frac{3}{4}\right]-\frac{2m_t^2}{s_{t\bar{b}}}-\frac{\pi^2}{3}+\frac{7}{2}-\ln^2\frac{2s_{min}}{s_{t\bar{b}}}\right\} \end{aligned} \tag{89}$$

4. Collinear singularities of $W\to t\bar{b}q\bar{q}$

Now let us consider the last piece of the real emission correction, $W^+\to t\bar{b}q\bar{q}$, which only involves the collinear divergence. We split the phase space into two parts,

$$\Theta\left(s_{q\bar{q}}-s_{min}\right)+\Theta\left(s_{min}-s_{q\bar{q}}\right), \tag{90}$$

where the first (second) term represents the finite (collinear) region, respectively. In the collinear region $q\parallel\bar{q}$, the matrix element square can factorized as

$$\left|\mathcal{M}\left(t\bar{b}q\bar{q}\right)\right|^2\xrightarrow{q\parallel\bar{q}}\frac{g_s}{2}f^{q\bar{q}\to g}\left|\mathcal{M}_0\right|^2, \tag{91}$$

where

$$f^{q\bar{q}\to g}\left(\xi\right)=\frac{2}{s_{q\bar{q}}}\frac{\xi^2+\left(1-\xi\right)^2-\epsilon}{1-\epsilon}. \tag{92}$$

Integration over the collinear region gives rise to the following collinear factor

$$C^{q\bar{q}\to g}=\frac{\alpha_s}{4\pi}\frac{1}{\Gamma(1-\epsilon)}\left(\frac{4\pi\mu^2}{s_{min}}\right)^{\epsilon}\left\{-\frac{2}{3\epsilon_{IR}}-\frac{10}{9}\right\}\times n_f, \tag{93}$$

where n_f denotes the light quark flavors.

D. complete result of the IR singularities of the real emission corrections

The complete soft and collinear singularities of the real emission corrections to the process $gb\to tW$ are given by

$$\hat{\sigma}_{IR}\;=\;\left(I_S+I_C\right)\left|\mathcal{M}_0\right|^2, \tag{94}$$

where the soft factor I_S is given by

$$\begin{aligned} I_S\;=\;\frac{1}{2}\Big[& I^{soft}\left(t,g_1,\bar{b}\right)+I^{soft}\left(t,g_2,\bar{b}\right)+I^{soft}\left(t,g_2,g_1\right) \\ & +I^{soft}\left(g_2,g_1,\bar{b}\right)+I^{soft}\left(t,g_1,\bar{b}\right)+I^{soft}\left(t,g_2,\bar{b}\right)\Big], \end{aligned} \tag{95}$$

while the collinear factor I_C is given by

$$I_C \;=\; \frac{1}{2}\left[C_{\mathcal{M}_1}^{gg\to g} + C_{\mathcal{M}_1}^{qg\to q} + C_{\mathcal{M}_2}^{gg\to g} + C_{\mathcal{M}_2}^{qg\to q} + C_{\mathcal{M}_{1+2}}^{qg_1\to q} + C_{\mathcal{M}_{1+2}}^{qg_2\to q}\right] + C^{q\bar{q}\to g}. \tag{96}$$

The factor "2" in above equations accounts for the two identical gluons in the final state. After summing over both soft and collinear factors, we obtain the IR divergences of the real emission corrections as following

$$\begin{aligned}\hat{\sigma}_{IR} \;=\; \frac{\alpha_s}{4\pi}C_\epsilon\Bigg\{ & \frac{26}{3\epsilon_{IR}^2} - \frac{6}{\epsilon_{IR}}\ln\frac{s_{tg}}{m_t^2} - \frac{6}{\epsilon_{IR}}\ln\frac{s_{g\bar{b}}}{m_t^2} + \frac{2}{\epsilon_{IR}}\ln\frac{s_{t\bar{b}}}{m_t^2} \\ & + \frac{1}{\epsilon_{IR}}\left(11 - \frac{2}{3}n_f\right) + \frac{20}{3\epsilon_{IR}} + \text{finite}\Bigg\}\left|\mathcal{M}_0\right|^2.\end{aligned} \tag{97}$$

It is clear that the IR divergences in the real emission corrections exactly cancel the UV divergences in the virtual corrections after we cross the gluon and bottom quark into the initial state and the W-boson to the final state, i.e.

$$s_{tg} \to -t_1, \qquad s_{g\bar{b}} \to s, \qquad s_{t\bar{b}} \to m_t^2 - m_W^2 - u. \tag{98}$$

VI. RESOLVED REAL EMISSION CORRECTIONS

The real emission corrections in the resolved phase phase region are finite and thus can be calculated numerically in 4 dimensions, using the canonical Monte Carlo method. With the implement of the phase space slicing conditions described above, the integration will depend upon the input value of s_{min}. Since the cutoff s_{min} is introduced in the calculation only for a technical reason and is unrelated to any physical quantity, the inclusive rate must not depend on it. In other words, the sum of all contributions, virtual, resolved, and unresolved corrections must be independent of s_{min}. This is the case as long as s_{min} is small enough so that the soft and collinear approximations are valid. However, numerical cancellation in the Monte Carlo integration becomes unstable if s_{min} is too small. Furthermore, the jet-finding algorithm and other infrared-safe experimental observables should also be defined in a way such that they are consistent with the choice of s_{min}. In practice, one wants to choose the largest s_{min} possible within these constraints in order to minimize the processing time of the Monte Carlo integration program. Since the phase space slicing conditions highly depend on the kinematics of the final state particles, it is better to calculate the resolved real emission corrections term by term in Eq. 50 to achieve better cancellation of the s_{min} dependence.

VII. CONCLUSION

In this paper we present a detailed calculation of the NLO QCD corrections to the tW associated production using the one cutoff phase space slicing method. The corrections to the this process have been calculated independently by two groups [28, 35], a number of differences were found. Therefore, a third party calculation is needed to make a crossing check. Furthermore, the fully analytic expression is still missing in the literature. In this note, we first calculated the virtual corrections using the dimensional regularization. The final results are shown completely in terms of the Passarino-Veltman scalar functions. We then use the one cutoff phase space slicing method to calculate the infrared singularities of the real emission corrections. The soft and collinear factorizations of the color ordered amplitudes are shown in details. The phenomenology study will be presented in the forthcoming paper.

Acknowledgments

We gratefully acknowledge stimulating discussions with Chuan-Ren Chen and C.-P. Yuan. This work is supported in part by the U. S. Department of Energy under Grant No. DE-FG03-94ER40837.

APPENDIX A: USEFUL FORMULA

The integration over the soft and collinear regions can be easily evaluated. Below we list the useful formula in our calculation [57]. All the integrals we need are of the form

$$I^{(k,l)} = \int_0^\pi \mathrm{d}\theta_1 \frac{\sin^{1-2\epsilon}\theta_1}{(a+b\cos\theta_1)^k} \int_0^\pi \mathrm{d}\theta_2 \frac{\sin^{-2\epsilon}\theta_2}{(A+B\cos\theta_1+C\sin\theta_1\cos\theta_2)^l}. \tag{A1}$$

The first point to notice is that there are four classes of integrals, depending on the collinear structure. The $[ab]$ and $[AB]$ variable can both be either "collinear" or not, which yields four combinations. In the case of the $[ab]$ variable, collinear divergence appears when $a^2 = b^2$ so that $(a + b\cos\theta_1) \to a(1 \pm \cos\theta_1)$. Then the zero occurs at the edge of the θ_1 integration region and is not integrable. For the $[ABC]$ variable the same comments apply for θ_2 when $A^2 = B^2 + C^2$. For our needs, the soft eikonal factor does not involve the angle θ_2, therefore the integration becomes more simpler.

When $A^2 \neq B^2 + C^2$, and $b = -a$, we use

$$
\begin{aligned}
I^{(1,1)} \;=\; & \frac{\pi}{a(A+B)} \left\{ -\frac{1}{\epsilon} + \ln\left[\frac{(A+B)^2}{A^2-B^2-C^2}\right] \right. \\
& -\epsilon \left[\ln^2\left(\frac{A-\sqrt{B^2+C^2}}{A+B}\right) - \frac{1}{2}\ln^2\left(\frac{A+\sqrt{B^2+C^2}}{A-\sqrt{B^2+C^2}}\right) \right. \\
& \left. \left. +2\mathrm{Li}_2\left(-\frac{B+\sqrt{B^2+C^2}}{A-\sqrt{B^2+C^2}}\right) - 2\mathrm{Li}_2\left(\frac{B-\sqrt{B^2+C^2}}{A+B}\right) \right] \right\} + \mathcal{O}(\epsilon^2), \quad \text{(A2)}
\end{aligned}
$$

While when $b \neq -a$ we use

$$
\begin{aligned}
I^{(0,1)} \;=\; & \frac{\pi}{\sqrt{B^2+C^2}} \left\{ \ln\left(\frac{A+\sqrt{B^2+C^2}}{A-\sqrt{B^2+C^2}}\right) \right. \\
& \left. +2\epsilon \left[\mathrm{Li}_2\left(\frac{2\sqrt{B^2+C^2}}{A+\sqrt{B^2+C^2}}\right) + \frac{1}{4}\ln^2\left(\frac{A+\sqrt{B^2+C^2}}{A-\sqrt{B^2+C^2}}\right) \right] \right\} + \mathcal{O}(\epsilon^2), \quad \text{(A3)} \\
I^{(0,2)} \;=\; & \frac{2\pi}{A^2-B^2-C^2} \left[1 + \epsilon \frac{A}{\sqrt{B^2+C^2}} \ln\left(\frac{A+\sqrt{B^2+C^2}}{A-\sqrt{B^2+C^2}}\right) \right]. \quad \text{(A4)}
\end{aligned}
$$

Finally, when $A = B^2 + C^2$, and $b = -a$, we have

$$
I^{(1,1)} = -\frac{1}{\epsilon}\frac{\pi}{aA}\left(\frac{A+B}{2A}\right)^{-1-\epsilon}\left[1 + \epsilon^2 \mathrm{Li}_2\left(\frac{A-B}{2A}\right)\right]. \quad \text{(A5)}
$$

APPENDIX B: PASSIANO-VELTMAN SCALAR FUNCTIONS

Here we list out the scalar functions used in this calculation. The general scalar functions are defined as follows:

$$
\begin{aligned}
& A_0\left(m^2\right) = \mu^{2\epsilon} \int \frac{d^n q}{(2\pi)^n} \frac{1}{q^2 - m^2}, \quad \text{(B1)} \\
& B_0\left(p_1^2; m_1^2, m_2^2\right) = \mu^{2\epsilon} \int \frac{d^n q}{(2\pi)^n} \frac{1}{\left[q^2 - m_1^2\right]\left[(q+p_1)^2 - m_2^2\right]}, \quad \text{(B2)} \\
& C_0\left(p_1^2, p_2^2, p_3^2; m_1^2, m_2^2, m_3^2\right) \\
& = \mu^{2\epsilon} \int \frac{d^n q}{(2\pi)^n} \frac{1}{\left[q^2 - m_1^2\right]\left[(q+p_1)^2 - m_2^2\right]\left[(q+p_1+p_2)^2 - m_3^2\right]}, \quad \text{(B3)} \\
& D_0\left(p_1^2, p_2^2, p_3^2, p_4^2; s_{12}, s_{23}; m_1^2, m_2^2, m_3^2, m_4^2\right) \quad \text{(B4)} \\
& = \mu^{2\epsilon} \int \frac{d^n q}{(2\pi)^n} \frac{1}{\left[q^2 - m_1^2\right]\left[(q+p_1)^2 - m_2^2\right]\left[(q+p_1+p_2)^2 - m_3^2\right]\left[(q+p_1+p_2+p_3)^2 - m_4^2\right]},
\end{aligned}
$$

where $n = 4 - 2\epsilon$, μ is the scale introduced so that the integrals preserve their natural dimensions. We follow the notation of Ref. [54] to calculate the scalar integrals in the

spacelike region, $p_i^2 < 0$ and $s_{ij} \equiv (p_i + p_j)^2 < 0$. The analytic continuation is performed by restoring the $i\varepsilon$,

$$p_i^2 \to p_i^2 + i\varepsilon, \quad s_{ij} \to s_{ij} + i\varepsilon, \quad m_i^2 \to m_i^2 - i\varepsilon.$$

The divergent three-point scalar functions used in this work are given as follows:

$$\begin{aligned}
&C_0^{V_i}\left(0,0,p_3^2;0,0,0\right) \\
&= \frac{1}{16\pi^2} C_\epsilon \left\{ \frac{1}{\epsilon^2} - \frac{1}{\epsilon} \ln\left(\frac{-p_3^2}{m_t^2}\right) + \frac{1}{2}\ln^2\left(\frac{-p_3^2}{m_t^2}\right) - \frac{1}{6}\pi^2 \right\}, \qquad \text{(B5)} \\
&C_0^{V_i}\left(0,p_2^2,m_t^2;0,0,m_t^2\right) \\
&= \frac{1}{16\pi^2} C_\epsilon \left\{ \frac{1}{2\epsilon^2} + \frac{1}{\epsilon} \ln\left(\frac{m_t^2}{m_t^2 - p_2^2}\right) + \frac{1}{2}\ln^2\left(\frac{m_t^2}{m_t^2 - p_2^2}\right) - \mathrm{Li}_2\left(\frac{-p_2^2}{m_t^2 - p_2^2}\right) \right\}, \qquad \text{(B6)} \\
&C_0^{V_i}\left(0,p_2^2,p_3^2;0,0,m_t^2\right) \\
&= \frac{1}{16\pi} C_\epsilon \frac{1}{p_2^2 - p_3^2} \left\{ \frac{1}{\epsilon} \ln\left(\frac{m_t^2 - p_3^2}{m_t^2 - p_2^2}\right) + \mathrm{Li}_2\left(\frac{p_2^2}{m_t^2}\right) - \mathrm{Li}_2\left(\frac{p_3^2}{m_t^2}\right) \right. \\
&\qquad \left. + \ln^2\left(\frac{m_t^2 - p_2^2}{m_t^2}\right) - \ln^2\left(\frac{m_t^2 - p_3^2}{m_t^2}\right) \right\}. \qquad \text{(B7)}
\end{aligned}$$

where

$$C_\epsilon \equiv \left(\frac{4\pi\mu^2}{m_t^2}\right)^\epsilon \Gamma\left(1+\epsilon\right).$$

The divergent four-point scalar functions are given as follows:

$$\begin{aligned}
&D_0^{B_1}\left(0,m_t^2,0,m_W^2;u,t;0,0,m_t^2,m_t^2\right) \\
&= \frac{1}{16\pi^2} C_\epsilon \frac{1}{(u-m_t^2)(t-m_t^2)} \left\{ \frac{1}{2\epsilon^2} - \frac{1}{\epsilon} \ln\left[\frac{(m_t^2-u)(m_t^2-t)}{(m_t^2-m_W^2)m_t^2}\right] - \frac{\pi^2}{6} \right. \\
&\qquad - \ln^2\left(\frac{m_t^2-m_W^2}{m_t^2}\right) + 2\ln\left(\frac{m_t^2-t}{m_t^2-m_W^2}\right)\ln\left(\frac{m_t^2-u}{m_t^2}\right) \\
&\qquad \left. -2\mathrm{Li}_2\left(1-\frac{m_t^2-m_W^2}{m_t^2-t}\right) - 2\mathrm{Li}_2\left(1-\frac{m_t^2-m_W^2}{m_t^2-u}\right) \right\}, \qquad \text{(B8)} \\
&D_0^{B_2}\left(0,0,m_t^2,m_W^2;s,u;0,m_t^2,0,0\right) \\
&= \frac{1}{16\pi^2} C_\epsilon \frac{1}{s\,(u-m_t^2)} \left\{ \frac{3}{2}\frac{1}{\epsilon^2} - \frac{1}{\epsilon}\left[2\ln\left(1-\frac{u}{m_t^2}\right) + \ln\left(\frac{s}{m_t^2}\right) - \ln\left(1-\frac{m_W^2}{m_t^2}\right)\right] \right. \\
&\quad \left. -2\mathrm{Li}_2\left(\frac{u-m_W^2}{u-m_t^2}\right) + 2\ln\left(\frac{-s}{m_t^2}\right)\ln\left(1-\frac{u}{m_t^2}\right) - \ln^2\left(1-\frac{m_W^2}{m_t^2}\right) - \frac{2}{3}\pi^2 \right\}, \qquad \text{(B9)} \\
&D_0^{B_3} = D_0^{B_2}\Big|_{u\to t}. \qquad \text{(B10)}
\end{aligned}$$

The scalar functions exhibit certain symmetries under interchange their arguments (either rotation or inversion). The symmetry properties of the triangle- and box-loop integrals used

in this calculation are listed as follows [54]:

(1) C_0-function

$$C_0\left(p_1^2,p_2^2,p_3^2;m_1^2,m_2^2,m_3^2\right) = C_0\left(p_2^2,p_3^2,p_1^2;m_2^2,m_3^2,m_1^2\right), \tag{B11}$$

$$C_0\left(p_1^2,p_2^2,p_3^2;m_1^2,m_2^2,m_3^2\right) = C_0\left(p_3^2,p_2^2,p_1^2;m_3^2,m_2^2,m_1^2\right). \tag{B12}$$

(2) D_0-function

$$\begin{aligned} & D_0\left(p_1^2,p_2^2,p_3^2,p_4^2;s_{12},s_{23};m_1^2,m_2^2,m_3^2,m_4^2\right) \\ = \; & D_0\left(p_2^2,p_3^2,p_4^2,p_1^2;s_{23},s_{12};m_2^2,m_3^2,m_4^2,m_1^2\right), \end{aligned} \tag{B13}$$

$$\begin{aligned} & D_0\left(p_1^2,p_2^2,p_3^2,p_4^2;s_{12},s_{23};m_1^2,m_2^2,m_3^2,m_4^2\right) \\ = \; & D_0\left(p_4^2,p_3^2,p_2^2,p_1^2;s_{12},s_{23};m_1^2,m_4^2,m_3^2,m_2^2\right). \end{aligned} \tag{B14}$$

APPENDIX C: FORM FACTORS OF THE VIRTUAL CORRECTIONS

- The form factors of the triangle loop V_1

$$f_2^{V_1} = \frac{1}{t_1}\Big\{2C_0m_tt_1+2m_tC_{11}t_1\Big\}, \tag{C1}$$

$$f_6^{V_1} = \frac{1}{t_1}\Big\{8C_0m_t^2+8m_t^2C_{11}-4m_t^2C_{21}+8C_{24}\Big\}, \tag{C2}$$

$$\begin{aligned} f_{12}^{V_1} = \frac{1}{t_1}\Big\{ & 2C_0\left(2m_t^2+t_1\right)+2\left(4m_t^2+t_1\right)C_{11}+2t_1C_{12} \\ & +2m_t^2C_{21}+2t_1C_{23}+4C_{24}\Big\}, \end{aligned} \tag{C3}$$

$$f_{16}^{V_1} = \frac{1}{t_1}\Big\{4m_tC_{11}+4m_tC_{21}\Big\}, \tag{C4}$$

where the arguments of the scalar function and tensor coefficients are $\left((-p_t)^2,p_g^2,(p_t-p_g)^2;0,m_t^2,m_t^2\right)=(m_t^2,0,t;0,m_t^2,m_t^2)$.

- The form factors of the triangle loop V_2

$$f_2^{V_2} = \frac{1}{t_1}\Big\{3C_0m_tt_1+3m_tC_{11}t_1\Big\}, \tag{C5}$$

$$\begin{aligned} f_6^{V_2} = \frac{1}{t_1}\Big\{ & 12C_0m_t^2+12C_{21}m_t^2+2\left(12m_t^2+t_1\right)C_{11}+4t_1C_{12}+8t_1C_{23}+24C_{24} \\ & +\epsilon\left(-8C_0m_t^2-16C_{11}m_t^2-8C_{21}m_t^2-4t_1C_{12}-4t_1C_{23}-16C_{24}\right)\Big\}, \end{aligned} \tag{C6}$$

$$f_{12}^{V_2} = \frac{1}{t_1}\Big\{6C_0m_t^2 + 2C_{21}m_t^2 + 2\left(4m_t^2+t_1\right)C_{11} + t_1C_{12} + 2t_1C_{23} + 12C_{24} - 8\epsilon C_{24}\Big\}, \quad \text{(C7)}$$

$$f_{16}^{V_2} = \frac{1}{t_1}\Big\{-4m_tC_{11} - 4m_tC_{21} + \epsilon\left(4C_0m_t + 8C_{11}m_t + 4C_{21}m_t\right)\Big\}, \quad \text{(C8)}$$

where the arguments of the scalar function and tensor coefficients are $\left((-p_2)^2, p_g^2, (p_t-p_g)^2; m_t^2, 0, 0\right) = (m_t^2, 0, t; m_t^2, 0, 0)$.

- The form factors of the triangle loop V_3:

$$f_6^{V_3} = \frac{1}{t_1}\Big\{4C_0\left(m_t^2 - m_W^2 + t_1\right) + 4\left(m_t^2 - m_W^2 + t_1\right)C_{11} + 4\left(m_t^2+t_1\right)C_{12} + 4m_W^2C_{22} + 4\left(m_t^2 - m_W^2 + t_1\right)C_{23} + 8C_{24} - 16C_{24}\epsilon\Big\}, \quad \text{(C9)}$$

$$f_9^{V_3} = \frac{1}{t_1}\Big\{-8m_tC_{12} + 8\epsilon m_tC_{23} - 8m_tC_{23}\Big\}, \quad \text{(C10)}$$

$$f_{12}^{V_3} = \frac{1}{t_1}\Big\{2C_0\left(m_t^2 - m_W^2 + t_1\right) + 2\left(m_t^2 - m_W^2 + t_1\right)C_{11} + 2\left(m_t^2+t_1\right)C_{12} + 2m_W^2C_{22} + 2\left(m_t^2 - m_W^2 + t_1\right)C_{23} + 4C_{24} - 8C_{24}\epsilon\Big\}, \quad \text{(C11)}$$

$$f_{13}^{V_3} = \frac{1}{t_1}\Big\{-4m_tC_{12} - 4m_tC_{23}\Big\}, \quad \text{(C12)}$$

where the arguments of the scalar function and tensor coefficients are $\left(p_b^2, (-p_W)^2, (p_W-p_b)^2; 0, 0, m_t^2\right) = (0, m_W^2, t; 0, 0, m_t^2)$.

- The form factors of the triangle loop V_1' ($f_i^{V_1'} \equiv F_i^{V_1'}/s$)

$$f_4^{V_1'} = (8C_{24} - 16C_{24}\epsilon)/s, \quad \text{(C13)}$$

$$f_5^{V_1'} = 4C_0 + 4C_{11} + 4C_{12} + 4C_{23} + 8C_{24}/s + \left(-4C_{12} - 4C_{23} - 16C_{24}/s\right)\epsilon, \quad \text{(C14)}$$

$$f_{11}^{V_1'} = -4C_0 - 4C_{11} - 4C_{12} - 4C_{23} - 8C_{24}/s + \left(4C_{12} + 4C_{23} + 16C_{24}/s\right)\epsilon, \quad \text{(C15)}$$

$$f_{12}^{V_1'} = 2C_0 + 2C_{11} + 2C_{12} + 2C_{23} + 4C_{24}/s + \left(-2C_{12} - 2C_{23} - 8C_{24}/s\right)\epsilon, \quad \text{(C16)}$$

where the arguments of the scalar function and tensor coefficients are $\left(p_b^2, p_g^2, (p_b+p_g)^2, 0, 0, 0\right) = (0, 0, s; 0, 0, 0)$.

- The form factors of the triangle loop V_2':

$$f_4^{V_2'} = 2C_{11} + 4C_{12} + 8C_{23} + 24C_{24}/s + \epsilon\left(-4C_{12} - 4C_{23} - 16C_{24}/s\right), \quad \text{(C17)}$$

$$f_5^{V_2'} = 4C_{11} + 2C_{12} + 4C_{23} + 24C_{24}/s - 16\epsilon C_{24}/s, \quad \text{(C18)}$$

$$f_{11}^{V_2'} = -4C_{11} - 2C_{12} - 4C_{23} - 24C_{24}/s + 16\epsilon C_{24}/s, \quad \text{(C19)}$$

$$f_{12}^{V_2'} = 2C_{11} + C_{12} + 2C_{23} + 12C_{24}/s - 8\epsilon C_{24}/s, \quad \text{(C20)}$$

where the arguments of the scalar function and tensor coefficients are $\left(p_b^2, p_g^2, (p_b + p_g)^2, 0, 0, 0\right) = (0, 0, s; 0, 0, 0)$.

- The form factors of the triangle loop V_3':

$$f_1^{V_3'} = \frac{1}{s}\Big\{4C_0 m_t + 4m_t C_{11}\Big\}, \quad \text{(C21)}$$

$$f_2^{V_3'} = -2C_0 m_t - 2m_t C_{11}, \quad \text{(C22)}$$

$$f_4^{V_3'} = \frac{1}{s}\Big\{4C_0\left(m_t^2 - m_W^2 + s\right) + 4\left(2m_t^2 - m_W^2 + s\right)C_{11} + \left(4s - 4m_t^2\right)C_{12} + 4m_t^2 C_{21} + 4m_W^2 C_{22} - 4\left(m_t^2 + m_W^2 - s\right)C_{23} + 8C_{24} - 16C_{24}\epsilon\Big\}, \quad \text{(C23)}$$

$$f_5^{V_3'} = \frac{1}{s}\Big\{4C_0\left(m_t^2 - m_W^2\right) + \left(8m_t^2 - 4m_W^2\right)C_{11} - 4m_t^2 C_{12} + 4m_t^2 C_{21} + 4m_W^2 C_{22} - 4\left(m_t^2 + m_W^2\right)C_{23} + 8C_{24} - 16C_{24}\epsilon\Big\}, \quad \text{(C24)}$$

$$f_8^{V_3'} = \frac{1}{s}\Big\{-8m_t C_{11} + 8m_t C_{12} - 8m_t C_{21} + 8m_t C_{23}\Big\}, \quad \text{(C25)}$$

$$f_{11}^{V_3'} = \frac{1}{s}\Big\{-4C_0\left(m_t^2 - m_W^2 + s\right) - 4\left(2m_t^2 - m_W^2 + s\right)C_{11} + 4\left(m_t^2 - s\right)C_{12} - 4m_t^2 C_{21} - 4m_W^2 C_{22} + 4\left(m_t^2 + m_W^2 - s\right)C_{23} - 8C_{24} + 16C_{24}\epsilon\Big\}, \quad \text{(C26)}$$

$$f_{12}^{V_3'} = \frac{1}{s}\Big\{2C_0\left(m_t^2 - m_W^2 + s\right) + 2\left(2m_t^2 - m_W^2 + s\right)C_{11} + \left(2s - 2m_t^2\right)C_{12} + 2m_t^2 C_{21} + 2m_W^2 C_{22} - 2\left(m_t^2 + m_W^2 - s\right)C_{23} + 4C_{24} - 8C_{24}\epsilon\Big\}, \quad \text{(C27)}$$

$$f_{15}^{V_3'} = \frac{1}{s}\Big\{-4m_t C_{11} + 4m_t C_{12} - 4m_t C_{21} + 4m_t C_{23}\Big\}, \quad \text{(C28)}$$

where the arguments of the scalar function and tensor coefficients are $\left((-p_t)^2, (-p_W)^2, (p_t + p_W)^2, 0, m_t^2, 0\right) = (m_t^2, m_W^2, s; 0, m_t^2, 0)$.

- The form factors of the box loop B_1:

$$
\begin{aligned}
f_1^{B_1} &= m_t\Big\{4\left(2m_t^2+t_1\right)D_{21}+4\left(m_t^2+m_W^2+t_1\right)D_{23}+4t_1D_{24}\\
&\quad -4\left(3m_t^2+m_W^2+2t_1\right)D_{25}-4t_1D_{26}+16D_{27}+4D_{31}m_t^2-4m_W^2D_{33}\\
&\quad +4t_1D_{34}-4\left(2m_t^2+m_W^2-s\right)D_{35}+4\left(m_t^2+2m_W^2-s\right)D_{37}\\
&\quad +4\left(s+t_1\right)D_{39}-4\left(s+2t_1\right)D_{310}+16D_{311}-16D_{313}\Big\}, \qquad \text{(C29)}\\
f_2^{B_1} &= m_t\Big\{-2sD_{11}+2sD_{13}-2\left(2m_t^2+t_1\right)D_{21}-2\left(m_t^2+m_W^2+t_1\right)D_{23}\\
&\quad -2t_1D_{24}+2\left(3m_t^2+m_W^2+2t_1\right)D_{25}+2t_1D_{26}-8D_{27}-2D_{31}m_t^2\\
&\quad +2m_W^2D_{33}-2t_1D_{34}+2\left(2m_t^2+m_W^2-s\right)D_{35}-2\left(m_t^2+2m_W^2-s\right)D_{37}\\
&\quad -2\left(s+t_1\right)D_{39}+2\left(s+2t_1\right)D_{310}-12D_{311}+12D_{313}\\
&\quad +\epsilon\Big[-2D_{31}m_t^2-2\left(2m_t^2+t_1\right)D_{21}-2\left(m_t^2+m_W^2+t_1\right)D_{23}-2t_1D_{24}\\
&\quad +2\left(3m_t^2+m_W^2+2t_1\right)D_{25}+2t_1D_{26}-4D_{27}+2m_W^2D_{33}-2t_1D_{34}\\
&\quad +2\left(2m_t^2+m_W^2-s\right)D_{35}m_t-2\left(m_t^2+2m_W^2-s\right)D_{37}m_t-2\left(s+t_1\right)D_{39}m_t\\
&\quad +2\left(s+2t_1\right)D_{310}m_t-8D_{311}m_t+8D_{313}m_t\Big]+\epsilon^2\left(4D_{311}-4D_{313}\right)\Big\} \qquad \text{(C30)}\\
f_4^{B_1} &= -8m_t^2D_{11}-4t_1D_{12}+4\left(2m_t^2+t_1\right)D_{13}-4m_t^2D_{21}-4t_1D_{24}+4m_t^2D_{25}\\
&\quad +4t_1D_{26}-8D_{27}-8D_{313}+\epsilon\Big[-4D_{35}m_t^2+4t_1D_{23}-4t_1D_{25}+8D_{27}\\
&\quad -4m_W^2D_{33}+4\left(m_t^2+m_W^2-s\right)D_{37}+4\left(s+t_1\right)D_{39}-4t_1D_{310}\\
&\quad -16D_{313}\Big]+8D_{313}\epsilon^2, \qquad \text{(C31)}\\
f_5^{B_1} &= -4t_1D_{12}+4t_1D_{13}-4m_t^2D_{21}-4m_W^2D_{23}-4t_1D_{24}+4\left(m_t^2+m_W^2\right)D_{25}\\
&\quad +4t_1D_{26}-8D_{27}-8D_{311}+\epsilon\Big[-8D_{21}m_t^2-4D_{31}m_t^2+4t_1D_{22}+\left(8m_t^2-4t_1\right)D_{24}\\
&\quad +4\left(m_t^2+m_W^2\right)D_{25}-4\left(m_t^2+m_W^2\right)D_{26}+8D_{27}+4\left(m_t^2-t_1\right)D_{34}\\
&\quad +4\left(m_t^2+m_W^2-s\right)D_{35}+4t_1D_{36}-4m_W^2D_{37}-4\left(s+t_1\right)D_{38}+4m_W^2D_{39}\\
&\quad -4\left(m_t^2+m_W^2-2s-t_1\right)D_{310}-16D_{311}+16D_{312}\Big]\\
&\quad +8D_{312}\left(8D_{311}-8D_{312}\right)\epsilon^2 \qquad \text{(C32)}\\
f_6^{B_1} &= 4D_0\left(m_t^2-m_W^2+s+t_1\right)+\left(12m_t^2+8\left(-m_W^2+s+t_1\right)\right)D_{11}+\left(4t_1-4s\right)D_{12}\\
&\quad +\left(-8m_t^2+4m_W^2-8t_1\right)D_{13}+4\left(3m_t^2-m_W^2+s+t_1\right)D_{21}+4\left(m_t^2+m_W^2+t_1\right)D_{23}\\
&\quad +\left(8t_1-4s\right)D_{24}-8\left(2m_t^2+t_1\right)D_{25}-8t_1D_{26}+16D_{27}+4m_t^2D_{31}-4m_W^2D_{33}
\end{aligned}
$$

$$
\begin{aligned}
&+4t_1 D_{34} - 4\left(2m_t^2 + m_W^2 - s\right) D_{35} + 4\left(m_t^2 + 2m_W^2 - s\right) D_{37} + 4\left(s + t_1\right) D_{39} \\
&-4\left(s + 2t_1\right) D_{310} + 16 D_{311} - 16 D_{313} \\
&+\left(4D_{21} m_t^2 + 4D_{23} m_t^2 - 4\left(2m_t^2 + s\right) D_{25} + 4sD_{26} - 8D_{27}\right)\epsilon + 8D_{27}\epsilon^2 \qquad \text{(C33)}
\end{aligned}
$$

$$
f_7^{B_1} = 8m_t\Big\{ D_{23} - 2D_{25} + D_{26} + D_{39} - D_{310} + \epsilon\left(D_{310} - D_{39}\right)\Big\} \qquad \text{(C34)}
$$

$$
f_8^{B_1} = 8m_t\Big\{ D_{25} - D_{26} - D_{35} + D_{37} - D_{39} + D_{310} + \epsilon\left(D_{35} - D_{37} + D_{39} - D_{310}\right)\Big\}, \qquad \text{(C35)}
$$

$$
\begin{aligned}
f_9^{B_1} = 8m_t\Big\{ &-D_{11} + D_{12} - 2D_{21} - D_{23} + 3D_{25} - D_{34} - D_{39} + 2D_{310} \\
&+\epsilon\left(D_{24} - D_{26} + D_{34} + D_{39} - 2D_{310}\right)\Big\}, \qquad \text{(C36)}
\end{aligned}
$$

$$
\begin{aligned}
f_{10}^{B_1} = 8m_t\Big\{ &-D_{12} + D_{13} - D_{31} + D_{34} + 2D_{35} - D_{37} + D_{39} - 2D_{310} \\
&+\epsilon\left(D_{21} - D_{24} - D_{25} + D_{26} + D_{31} - D_{34} - 2D_{35} + D_{37} - D_{39} + 2D_{310}\right)\Big\}, \qquad \text{(C37)}
\end{aligned}
$$

$$
\begin{aligned}
f_{11}^{B_1} = &\, 4D_{21} m_t^2 - 8D_{24} m_t^2 - 4t_1 D_{22} - 4\left(m_t^2 + t_1\right) D_{23} + 4\left(m_t^2 - m_W^2 + s + t_1\right) D_{25} \\
&+4\left(m_t^2 + m_W^2 - s + t_1\right) D_{26} - 16\epsilon D_{27} + 4m_W^2 D_{33} - 4D_{34} m_t^2 + 4D_{35} m_t^2 \\
&-4t_1 D_{36} - 4\left(m_t^2 + m_W^2 - s\right) D_{37} + 4\left(s + t_1\right) D_{38} - 4\left(m_W^2 + s + t_1\right) D_{39} \\
&+4\left(m_t^2 + m_W^2 - s + t_1\right) D_{310} - 16 D_{312} + 16 D_{313} \qquad \text{(C38)}
\end{aligned}
$$

$$
\begin{aligned}
f_{12}^{B_1} = &\, 2D_0\left(m_t^2 - m_W^2 + s + t_1\right) + 2\left(2m_t^2 - m_W^2 + s + t_1\right) D_{11} - 2m_t^2 D_{13} - 2m_t^2 D_{21} \\
&+2t_1 D_{22} + 2\left(m_t^2 + t_1\right) D_{23} + 4m_t^2 D_{24} - 2\left(m_t^2 - m_W^2 + s + t_1\right) D_{25} \\
&-2\left(m_t^2 + m_W^2 - s + t_1\right) D_{26} + 4D_{27} - 2m_W^2 D_{33} + 2m_t^2 D_{34} - 2m_t^2 D_{35} \\
&+2t_1 D_{36} + 2\left(m_t^2 + m_W^2 - s\right) D_{37} - 2\left(s + t_1\right) D_{38} + 2\left(m_W^2 + s + t_1\right) D_{39} \\
&-2\left(m_t^2 + m_W^2 - s + t_1\right) D_{310} + 12 D_{312} - 12 D_{313} + \left(4D_{27} - 4D_{312} + 4D_{313}\right)\epsilon^2 \\
&+\epsilon\Big[-2D_{21} m_t^2 + 4D_{24} m_t^2 + 2D_{34} m_t^2 - 2D_{35} m_t^2 + 2t_1 D_{22} + 2\left(m_t^2 + t_1\right) D_{23} \\
&-2\left(m_t^2 - m_W^2 + s + t_1\right) D_{25} - 2\left(m_t^2 + m_W^2 - s + t_1\right) D_{26} + 8D_{27} - 2m_W^2 D_{33} \\
&+2t_1 D_{36} + 2\left(m_t^2 + m_W^2 - s\right) D_{37} - 2\left(s + t_1\right) D_{38} + 2\left(m_W^2 + s + t_1\right) D_{39} \\
&-2\left(m_t^2 + m_W^2 - s + t_1\right) D_{310} + 8D_{312} - 8D_{313}\Big] \qquad \text{(C39)}
\end{aligned}
$$

$$
f_{13}^{B_1} = -4m_t D_{11} + 4m_t D_{12} + 4m_t D_{24} - 4m_t D_{26} + \epsilon\left(4m_t D_{24} - 4m_t D_{26}\right) \qquad \text{(C40)}
$$

$$
f_{14}^{B_1} = 4m_t D_{11} - 4m_t D_{13} - 4m_t D_{25} + \epsilon\left(4m_t D_{23} - 4m_t D_{25}\right) + 4m_t D_{26} \qquad \text{(C41)}
$$

$$
\begin{aligned}
f_{15}^{B_1} = &-4m_t D_{12} + 4m_t D_{13} + 4m_t D_{21} - 4m_t D_{24} - 4m_t D_{25} + 4m_t D_{26} \\
&+\epsilon\left(4m_t D_{21} - 4m_t D_{24} - 4m_t D_{25} + 4m_t D_{26}\right) \qquad \text{(C42)}
\end{aligned}
$$

$$
\begin{aligned}
f_{16}^{B_1} &= 4m_tD_{12} - 4m_tD_{13} - 4m_tD_{21} + 4m_tD_{24} + 4m_tD_{25} \\
&\quad +\epsilon\left(-4m_tD_{21} - 4m_tD_{23} + 8m_tD_{25}\right) - 4m_tD_{26} \qquad \text{(C43)} \\
f_{17}^{B_1} &= -8D_{23} + 8D_{26} + 8D_{38} - 8D_{39} + \epsilon\left(8D_{23} - 8D_{26} - 8D_{38} + 8D_{39}\right) \qquad \text{(C44)} \\
f_{18}^{B_1} &= -8D_{25} + 8D_{26} - 8D_{37} - 8D_{38} + 8D_{39} \\
&\quad +\epsilon\left(-8D_{25} + 8D_{26} + 8D_{37} + 8D_{38} - 8D_{39} - 8D_{310}\right) + 8D_{310} \qquad \text{(C45)} \\
f_{19}^{B_1} &= 16D_{12} - 16D_{13} + 8D_{22} + 8D_{23} + 16D_{24} - 8D_{25} - 24D_{26} + 8D_{36} - 8D_{38} + 8D_{39} \\
&\quad -8D_{310} + \epsilon\left(-8D_{22} - 8D_{23} + 8D_{25} + 8D_{26} - 8D_{36} + 8D_{38} - 8D_{39} + 8D_{310}\right) \qquad \text{(C46)} \\
f_{20}^{B_1} &= -8D_{22} + 8D_{24} - 8D_{25} + 8D_{26} + 8D_{34} - 8D_{35} - 8D_{36} + 8D_{37} + 8D_{38} - 8D_{39} \\
&\quad +\epsilon\Big[8D_{22} - 8D_{24} + 8D_{25} - 8D_{26} - 8D_{34} + 8D_{35} + 8D_{36} \\
&\quad -8D_{37} - 8D_{38} + 8D_{39}\Big], \qquad \text{(C47)}
\end{aligned}
$$

where the arguments of the scalar function and tensor coefficients are $\left((-p_t)^2, p_g^2, (-p_W)^2, p_b^2; t, u; 0, m_t^2, m_t^2, 0\right) = (m_t^2, 0, m_W^2, 0; t, u; 0, m_t^2, m_t^2, 0)$.

- The form factors of the box loop B_2

$$
\begin{aligned}
f_1^{B_2} &= -4D_{21}m_t^3 - 4\left(m_t^2 - m_W^2 + t_1\right)D_{11}m_t + 4\left(m_t^2 - m_W^2 - s + t_1\right)D_{12}m_t + 4sD_{13}m_t \\
&\quad -4m_W^2D_{22}m_t + 4\left(m_t^2 + m_W^2 - s\right)D_{24}m_t - 4t_1D_{25}m_t + 4\left(s + t_1\right)D_{26}m_t - 8D_{27}m_t \\
&\quad -8D_{311}m_t + 8D_{312}m_t + \epsilon^2\left(8m_tD_{311} - 8m_tD_{312}\right) + \epsilon\Big[-4D_{31}m_t^3 \\
&\quad -4\left(m_t^2 - m_W^2 + s\right)D_{21}m_t + 4\left(-m_t^2 + m_W^2 + s\right)D_{22}m_t + 8\left(m_t^2 - m_W^2\right)D_{24}m_t \\
&\quad +4sD_{25}m_t - 4sD_{26}m_t + 8D_{27}m_t + 4m_W^2D_{32}m_t + 4\left(2m_t^2 + m_W^2 - s\right)D_{34}m_t \\
&\quad -4t_1D_{35}m_t - 4\left(m_t^2 + 2m_W^2 - s\right)D_{36}m_t - 4\left(s + t_1\right)D_{38}m_t + 4\left(s + 2t_1\right)D_{310}m_t \\
&\quad -16D_{311}m_t + 16D_{312}m_t\Big], \qquad \text{(C48)} \\
f_2^{B_2} &= 2D_{31}m_t^3 + 2\left(m_t^2 - m_W^2 + t_1\right)D_{11}m_t + 2\left(-m_t^2 + m_W^2 + s - t_1\right)D_{12}m_t - 2sD_{13}m_t \\
&\quad +2\left(2m_t^2 - m_W^2 + s\right)D_{21}m_t + 2\left(m_t^2 - s\right)D_{22}m_t + 2\left(-3m_t^2 + m_W^2 + s\right)D_{24}m_t \\
&\quad +2\left(t_1 - s\right)D_{25}m_t - 2t_1D_{26}m_t + 4D_{27}m_t - 2m_W^2D_{32}m_t - 2\left(2m_t^2 + m_W^2 - s\right)D_{34}m_t \\
&\quad +2t_1D_{35}m_t + 2\left(m_t^2 + 2m_W^2 - s\right)D_{36}m_t + 2\left(s + t_1\right)D_{38}m_t - 2\left(s + 2t_1\right)D_{310}m_t \\
&\quad +12D_{311}m_t - 12D_{312}m_t + \epsilon\Big[2D_{31}m_t^3 + 2\left(m_t^2 - m_W^2 + s\right)D_{21}m_t \\
&\quad +2\left(m_t^2 - m_W^2 - s\right)D_{22}m_t - 2sD_{25}m_t + 2sD_{26}m_t - 4D_{27}m_t - 2m_W^2D_{32}m_t \\
&\quad -2\left(2m_t^2 + m_W^2 - s\right)D_{34}m_t + 2t_1D_{35}m_t + 2\left(m_t^2 + 2m_W^2 - s\right)D_{36}m_t
\end{aligned}
$$

$$
\begin{aligned}
&+2\left(s+t_1\right)D_{38}m_t-2\left(s+2t_1\right)D_{310}m_t+8D_{311}m_t-8D_{312}m_t\\
&+\left(4m_tm_W^2-4m_t^3\right)D_{24}\Big]+\epsilon^2\left(4m_tD_{312}-4m_tD_{311}\right), \qquad \text{(C49)}\\
f_4^{B_2} &= 4D_0\left(m_t^2-m_W^2+s+t_1\right)+4\left(2m_t^2-m_W^2+s+t_1\right)D_{11}+\left(8s-4m_W^2\right)D_{12}\\
&+\left(4t_1-4s\right)D_{13}+4m_t^2D_{21}+4\left(-m_t^2+m_W^2+s\right)D_{22}+4\left(m_t^2-2m_W^2+2s\right)D_{24}\\
&+4t_1D_{25}-8sD_{26}+16D_{27}+4m_W^2D_{32}+4m_t^2D_{34}-4\left(m_t^2+m_W^2-s\right)D_{36}\\
&-4\left(s+t_1\right)D_{38}+4t_1D_{310}+16D_{312}\\
&+\left(-4D_{21}m_t^2-4D_{22}m_t^2+8D_{24}m_t^2-4t_1D_{25}+4t_1D_{26}-8D_{27}\right)\epsilon+8D_{27}\epsilon^2, \qquad \text{(C50)}\\
f_5^{B_2} &= 4D_0\left(m_t^2-m_W^2+s+t_1\right)+\left(12m_t^2+8\left(-m_W^2+s+t_1\right)\right)D_{11}\\
&+4\left(-2m_t^2+m_W^2+s-t_1\right)D_{12}-8sD_{13}+4\left(2m_t^2-m_W^2+s+t_1\right)D_{21}+4m_W^2D_{22}\\
&+4sD_{23}-4\left(2m_t^2-2s+t_1\right)D_{24}-4\left(m_t^2-m_W^2+2s\right)D_{25}+4\left(m_t^2-m_W^2-2s\right)D_{26}\\
&+16D_{27}+4m_t^2D_{31}-4\left(m_t^2+m_W^2-s\right)D_{34}+\left(4t_1-4m_t^2\right)D_{35}+4m_W^2D_{36}-4t_1D_{37}\\
&-4m_W^2D_{38}+4\left(s+t_1\right)D_{39}+4\left(m_t^2+m_W^2-2s-t_1\right)D_{310}+16D_{311}-16D_{313}\\
&+\left(-4D_{21}m_t^2-4m_W^2D_{22}+4\left(m_t^2+m_W^2\right)D_{24}-4t_1D_{25}+4t_1D_{26}-8D_{27}\right)\epsilon\\
&+8D_{27}\epsilon^2, \qquad \text{(C51)}\\
f_6^{B_2} &= -4sD_{12}+4sD_{13}-4sD_{24}+4sD_{26}-8D_{27}-8D_{311}+8D_{312}+\left(8D_{311}-8D_{312}\right)\epsilon^2\\
&+\epsilon\Big[-4D_{31}m_t^2+4sD_{22}-4sD_{24}+8D_{27}+4m_W^2D_{32}+4\left(2m_t^2+m_W^2-s\right)D_{34}\\
&-4t_1D_{35}-4\left(m_t^2+2m_W^2-s\right)D_{36}-4\left(s+t_1\right)D_{38}+4\left(s+2t_1\right)D_{310}\\
&-16D_{311}+16D_{312}\Big], \qquad \text{(C52)}\\
f_7^{B_2} &= -8m_tD_{12}+8m_tD_{13}-8m_tD_{24}-8m_tD_{25}+16m_tD_{26}+8m_tD_{38}-8m_tD_{310}\\
&+\epsilon\left(8m_tD_{22}-8m_tD_{24}+8m_tD_{25}-8m_tD_{26}-8m_tD_{38}+8m_tD_{310}\right), \qquad \text{(C53)}\\
f_8^{B_2} &= -8m_tD_{11}+16m_tD_{12}-8m_tD_{13}-8m_tD_{21}+8m_tD_{22}+8m_tD_{24}+8m_tD_{25}\\
&-16m_tD_{26}-8m_tD_{34}+8m_tD_{36}-8m_tD_{38}+8m_tD_{310}+\epsilon\Big[8m_tD_{21}-8m_tD_{22}\\
&-8m_tD_{25}+8m_tD_{26}+8m_tD_{34}-8m_tD_{36}+8m_tD_{38}-8m_tD_{310}\Big], \qquad \text{(C54)}\\
f_9^{B_2} &= -8m_tD_{21}+8m_tD_{24}+8m_tD_{25}-8m_tD_{26}-8m_tD_{35}-8m_tD_{38}+16m_tD_{310}\\
&+\epsilon\left(-8m_tD_{21}-8m_tD_{22}+16m_tD_{24}+8m_tD_{35}+8m_tD_{38}-16m_tD_{310}\right), \qquad \text{(C55)}\\
f_{10}^{B_2} &= -8m_tD_{22}+8m_tD_{24}-8m_tD_{25}+8m_tD_{26}-8m_tD_{31}+16m_tD_{34}+8m_tD_{35}\\
&-8m_tD_{36}+8m_tD_{38}-16m_tD_{310}+\epsilon\Big[8m_tD_{21}+8m_tD_{22}-16m_tD_{24}
\end{aligned}
$$

$$+8m_tD_{31} - 16m_tD_{34} - 8m_tD_{35} + 8m_tD_{36} - 8m_tD_{38} + 16m_tD_{310}\Big], \tag{C56}$$

$$\begin{aligned}
f_{11}^{B_2} &= \left(-8D_{27} + 8D_{312} - 8D_{313}\right)\epsilon^2 \\
&\quad +\epsilon\Big[4D_{21}m_t^2 - 8D_{24}m_t^2 - 4D_{34}m_t^2 + 4D_{35}m_t^2 + 4\left(m_t^2 - s\right)D_{22} - 4sD_{23} \\
&\quad +4\left(m_t^2 - m_W^2 + s + t_1\right)D_{25} - 4\left(m_t^2 - m_W^2 - s + t_1\right)D_{26} - 4m_W^2D_{32} \\
&\quad +4\left(m_t^2 + m_W^2 - s\right)D_{36} + 4t_1D_{37} + 4\left(m_W^2 + s + t_1\right)D_{38} - 4\left(s + t_1\right)D_{39} \\
&\quad -4\left(m_t^2 + m_W^2 - s + t_1\right)D_{310} - 16D_{312} + 16D_{313}\Big] \\
&\quad -4D_0\left(m_t^2 - m_W^2 + s + t_1\right) - 4\left(2m_t^2 - m_W^2 + s + t_1\right)D_{11} + 4m_t^2D_{12} \\
&\quad -8D_{27} - 8D_{312} + 8D_{313}
\end{aligned} \tag{C57}$$

$$\begin{aligned}
f_{12}^{B_2} &= \epsilon\Big[-2D_{21}m_t^2 + 4D_{24}m_t^2 + 2D_{34}m_t^2 - 2D_{35}m_t^2 + \left(2s - 2m_t^2\right)D_{22} + 2sD_{23} \\
&\quad -2\left(m_t^2 - m_W^2 + s + t_1\right)D_{25} + 2\left(m_t^2 - m_W^2 - s + t_1\right)D_{26} + 8D_{27} + 2m_W^2D_{32} \\
&\quad -2\left(m_t^2 + m_W^2 - s\right)D_{36} - 2t_1D_{37} - 2\left(m_W^2 + s + t_1\right)D_{38} + 2\left(s + t_1\right)D_{39} \\
&\quad +2\left(m_t^2 + m_W^2 - s + t_1\right)D_{310} + 8D_{312} - 8D_{313}\Big] \\
&\quad +2D_0\left(m_t^2 - m_W^2 + s + t_1\right) + 2\left(2m_t^2 - m_W^2 + s + t_1\right)D_{11} - 2m_t^2D_{12} - 2m_t^2D_{21} \\
&\quad +\left(2s - 2m_t^2\right)D_{22} + 2sD_{23} + 4m_t^2D_{24} - 2\left(m_t^2 - m_W^2 + s + t_1\right)D_{25} \\
&\quad +2\left(m_t^2 - m_W^2 - s + t_1\right)D_{26} + 4D_{27} + 2m_W^2D_{32} + 2m_t^2D_{34} - 2m_t^2D_{35} \\
&\quad -2\left(m_t^2 + m_W^2 - s\right)D_{36} - 2t_1D_{37} - 2\left(m_W^2 + s + t_1\right)D_{38} + 2\left(s + t_1\right)D_{39} \\
&\quad +2\left(m_t^2 + m_W^2 - s + t_1\right)D_{310} + 12D_{312} - 12D_{313} \\
&\quad +\left(4D_{27} - 4D_{312} + 4D_{313}\right)\epsilon^2
\end{aligned} \tag{C58}$$

$$f_{13}^{B_2} = -4m_tD_{11} + 4m_tD_{12} + 4m_tD_{25} - 4m_tD_{26} + \epsilon\left(4m_tD_{25} - 4m_tD_{26}\right) \tag{C59}$$

$$f_{14}^{B_2} = 4m_tD_{11} - 8m_tD_{12} + 4m_tD_{13} - 4m_tD_{24} + \epsilon\left(4m_tD_{22} - 4m_tD_{24}\right) + 4m_tD_{26} \tag{C60}$$

$$\begin{aligned}
f_{15}^{B_2} &= 4m_tD_{21} - 4m_tD_{24} - 4m_tD_{25} + 4m_tD_{26} \\
&\quad +\epsilon\left(4m_tD_{21} - 4m_tD_{24} - 4m_tD_{25} + 4m_tD_{26}\right)
\end{aligned} \tag{C61}$$

$$f_{16}^{B_2} = -4m_tD_{21} + 4m_tD_{24} + \epsilon\left(-4m_tD_{21} - 4m_tD_{22} + 8m_tD_{24}\right) + 4m_tD_{25} - 4m_tD_{26} \tag{C62}$$

$$f_{17}^{B_2} = 8D_{23} - 8D_{26} - 8D_{38} + \epsilon\left(-8D_{23} + 8D_{26} + 8D_{38} - 8D_{39}\right) + 8D_{39} \tag{C63}$$

$$\begin{aligned}
f_{18}^{B_2} &= -16D_{12} + 16D_{13} - 8D_{22} - 8D_{23} - 16D_{24} + 8D_{25} + 24D_{26} - 8D_{36} + 8D_{38} - 8D_{39} \\
&\quad +\epsilon\left(8D_{22} + 8D_{23} - 8D_{25} - 8D_{26} + 8D_{36} - 8D_{38} + 8D_{39} - 8D_{310}\right) + 8D_{310}
\end{aligned} \tag{C64}$$

$$f_{19}^{B_2} = 8D_{25} - 8D_{26} + 8D_{37} + 8D_{38} - 8D_{39} - 8D_{310}$$

$$+\epsilon\left(8D_{25}-8D_{26}-8D_{37}-8D_{38}+8D_{39}+8D_{310}\right) \tag{C65}$$

$$\begin{aligned} f_{20}^{B_2} &= 8D_{22}-8D_{24}+8D_{25}-8D_{26}-8D_{34}+8D_{35}+8D_{36}-8D_{37}-8D_{38}+8D_{39} \\ &+\epsilon\Big[-8D_{22}+8D_{24}-8D_{25}+8D_{26}+8D_{34}-8D_{35}-8D_{36} \\ &+8D_{37}+8D_{38}-8D_{39}\Big], \end{aligned} \tag{C66}$$

where the arguments of the scalar function and tensor coefficients are $\left((-p_t)^2,(-p_W)^2,p_g^2,p_b^2;s,u;0,m_t^2,0,0\right)=(m_t^2,m_W^2,0,0;s,u;0,m_t^2,0,0)$.

- The form factors of the box loop B_3:

$$\begin{aligned} f_1^{B_3} &= -4D_{21}m_t^3-2D_{31}m_t^3+4t_1D_{11}m_t-4t_1D_{12}m_t-2\left(m_t^2+m_W^2-s\right)D_{22}m_t \\ &+2\left(3m_t^2+m_W^2-s\right)D_{24}m_t+2\left(m_t^2-m_W^2+s+t_1\right)D_{25}m_t \\ &-2\left(m_t^2-m_W^2+s+t_1\right)D_{26}m_t-12D_{27}m_t+2m_W^2D_{32}m_t \\ &+2\left(2m_t^2+m_W^2-s\right)D_{34}m_t+2\left(m_t^2-m_W^2+s+t_1\right)D_{35}m_t \\ &-2\left(m_t^2+2m_W^2-s\right)D_{36}m_t+2\left(m_t^2-m_W^2+t_1\right)D_{38}m_t \\ &-2\left(2m_t^2-2m_W^2+s+2t_1\right)D_{310}m_t-4D_{311}m_t+4D_{312}m_t \\ &+\epsilon\left(4m_tD_{312}-4m_tD_{311}\right) \end{aligned} \tag{C67}$$

$$\begin{aligned} f_2^{B_3} &= 2m_tD_{22}m_W^2+m_t\left(s-2t_1\right)D_{11}-m_t\left(s-2t_1\right)D_{12}+m_t\left(m_t^2+m_W^2-s\right)D_{21} \\ &+m_t\left(-m_t^2-3m_W^2+s\right)D_{24}-m_t\left(m_t^2-m_W^2+t_1\right)D_{25} \\ &+m_t\left(m_t^2-m_W^2+t_1\right)D_{26}+6m_tD_{27} \end{aligned} \tag{C68}$$

$$\begin{aligned} f_4^{B_3} &= -4D_0t_1+4\left(m_t^2-t_1\right)D_{11}-2\left(3m_t^2-m_W^2+s\right)D_{12}+2\left(m_t^2-m_W^2+s+t_1\right)D_{13} \\ &+2m_t^2D_{21}+2\left(m_t^2-s\right)D_{22}-2\left(m_t^2-m_W^2+s+t_1\right)D_{23}-2\left(3m_t^2-m_W^2+s\right)D_{24} \\ &+2\left(m_t^2-m_W^2+s-t_1\right)D_{25}+2\left(m_t^2-m_W^2+2\left(s+t_1\right)\right)D_{26}-2m_W^2D_{32} \\ &-2m_t^2D_{34}+2m_t^2D_{35}+2\left(m_t^2+m_W^2-s\right)D_{36}-2\left(m_t^2-m_W^2+s+t_1\right)D_{37} \\ &-2\left(m_t^2-2m_W^2+t_1\right)D_{38}+2\left(m_t^2-m_W^2+t_1\right)D_{39}+\left(-4m_W^2+4s+2t_1\right)D_{310} \\ &-4D_{312}+4D_{313}+\epsilon\Big[4D_{34}m_t^2-4D_{35}m_t^2+4sD_{22}+4sD_{23}-8sD_{26} \\ &-4D_{27}+4m_W^2D_{32}-4\left(m_t^2+m_W^2-s\right)D_{36}+4\left(m_t^2-m_W^2+s+t_1\right)D_{37} \\ &+4\left(m_t^2-2m_W^2+t_1\right)D_{38}-4\left(m_t^2-m_W^2+t_1\right)D_{39}+\left(8m_W^2-4\left(2s+t_1\right)\right)D_{310} \\ &+20D_{312}-20D_{313}\Big]+\left(8D_{313}-8D_{312}\right)\epsilon^2 \end{aligned} \tag{C69}$$

$$f_5^{B_3} = 2D_{31}m_t^2-4D_0t_1+4\left(m_t^2-2t_1\right)D_{11}-2\left(m_t^2+m_W^2-s-2t_1\right)D_{12}$$

$$
\begin{aligned}
&-2\left(m_t^2-m_W^2+s+t_1\right)D_{13}+\left(10m_t^2-4t_1\right)D_{21}+6m_W^2D_{22}\\
&+4\left(-2m_t^2-2m_W^2+s+t_1\right)D_{24}-4\left(2m_t^2-2m_W^2+s+2t_1\right)D_{25}\\
&+6\left(m_t^2-m_W^2+t_1\right)D_{26}+28D_{27}-2\left(m_t^2+m_W^2-s\right)D_{34}\\
&-2\left(m_t^2-m_W^2+s+t_1\right)D_{35}+2m_W^2D_{36}+2\left(m_t^2-m_W^2+t_1\right)D_{310}\\
&+\epsilon\left(-20D_{27}-12D_{311}\right)+20D_{311} \qquad \text{(C70)}\\
f_6^{B_3} \;=\;& -2D_0s-2\left(m_t^2-m_W^2+2s\right)D_{11}+2\left(m_t^2-m_W^2+2s\right)D_{12}+2sD_{13}\\
&-2\left(2m_t^2-m_W^2+s\right)D_{21}+\left(2s-2m_t^2\right)D_{22}+2\left(3m_t^2-m_W^2+s\right)D_{24}\\
&+2\left(m_t^2-m_W^2+t_1\right)D_{25}-2\left(m_t^2-m_W^2+s+t_1\right)D_{26}-2m_t^2D_{31}+2m_W^2D_{32}\\
&+2\left(2m_t^2+m_W^2-s\right)D_{34}+2\left(m_t^2-m_W^2+s+t_1\right)D_{35}-2\left(m_t^2+2m_W^2-s\right)D_{36}\\
&+2\left(m_t^2-m_W^2+t_1\right)D_{38}-2\left(2m_t^2-2m_W^2+s+2t_1\right)D_{310}-4D_{311}+4D_{312}\\
&+\epsilon\Big[4D_{31}m_t^2-4sD_{22}+4sD_{24}-4sD_{25}+4sD_{26}-4D_{27}-4m_W^2D_{32}\\
&-4\left(2m_t^2+m_W^2-s\right)D_{34}-4\left(m_t^2-m_W^2+s+t_1\right)D_{35}\\
&+4\left(m_t^2+2m_W^2-s\right)D_{36}-4\left(m_t^2-m_W^2+t_1\right)D_{38}\\
&+4\left(2m_t^2-2m_W^2+s+2t_1\right)D_{310}+20D_{311}-20D_{312}\Big]\\
&+\left(8D_{312}-8D_{311}\right)\epsilon^2 \qquad \text{(C71)}\\
f_7^{B_3} \;=\;& 8m_tD_{12}-8m_tD_{13}+8m_tD_{24}-8m_tD_{25}+8m_tD_{37}+8m_tD_{38}\\
&-8m_tD_{39}-8m_tD_{310}+\epsilon\Big(-8m_tD_{22}+8m_tD_{24}-8m_tD_{25}\\
&+8m_tD_{26}-8m_tD_{37}-8m_tD_{38}+8m_tD_{39}+8m_tD_{310}\Big) \qquad \text{(C72)}\\
f_8^{B_3} \;=\;& -8m_tD_{12}+8m_tD_{13}-8m_tD_{22}+8m_tD_{26}+8m_tD_{34}-8m_tD_{35}\\
&-8m_tD_{36}+8m_tD_{310}+\epsilon\Big(8m_tD_{22}-8m_tD_{24}+8m_tD_{25}-8m_tD_{26}\\
&-8m_tD_{34}+8m_tD_{35}+8m_tD_{36}-8m_tD_{310}\Big) \qquad \text{(C73)}\\
f_9^{B_3} \;=\;& 8m_tD_{21}-8m_tD_{24}-8m_tD_{35}-8m_tD_{38}+16m_tD_{310}\\
&+\epsilon\left(8m_tD_{21}+8m_tD_{22}-16m_tD_{24}+8m_tD_{35}+8m_tD_{38}-16m_tD_{310}\right) \qquad \text{(C74)}\\
f_{10}^{B_3} \;=\;& 8m_tD_{22}-8m_tD_{24}+8m_tD_{31}-16m_tD_{34}+8m_tD_{36}\\
&+\epsilon\left(-8m_tD_{21}-8m_tD_{22}+16m_tD_{24}-8m_tD_{31}+16m_tD_{34}-8m_tD_{36}\right) \qquad \text{(C75)}\\
f_{11}^{B_3} \;=\;& -6D_{21}m_t^2-2D_{34}m_t^2+4D_0t_1+\left(4t_1-4m_t^2\right)D_{11}+2\left(m_t^2+m_W^2-3s\right)D_{12}\\
&+2\left(m_t^2-m_W^2+3s+t_1\right)D_{13}+2\left(m_t^2-2m_W^2-s\right)D_{22}+2\left(m_t^2+3m_W^2-3s\right)D_{24}
\end{aligned}
$$

$$+6\left(m_t^2-m_W^2+s+t_1\right)D_{25}+\left(-4m_t^2+4m_W^2+2s-4t_1\right)D_{26}-8D_{27}-2m_W^2D_{32}$$
$$+2\left(m_t^2+m_W^2-s\right)D_{36}-2\left(m_t^2-m_W^2+t_1\right)D_{38}+2\left(m_t^2-m_W^2+s+t_1\right)D_{310}$$
$$+\epsilon\left(12D_{27}-4D_{312}\right)-4D_{312} \tag{C76}$$

$$f_{12}^{B_3} = 5D_{21}m_t^2-2D_0t_1+2\left(m_t^2-t_1\right)D_{11}+\left(-m_t^2-m_W^2+4s\right)D_{12}$$
$$+\left(-m_t^2+m_W^2-3s-t_1\right)D_{13}+3m_W^2D_{22}-4\left(m_t^2+m_W^2-s\right)D_{24}$$
$$-5\left(m_t^2-m_W^2+s+t_1\right)D_{25}+4\left(m_t^2-m_W^2+t_1\right)D_{26}-14\epsilon D_{27}+6D_{27} \tag{C77}$$

$$f_{13}^{B_3} = 4m_tD_{11}-4m_tD_{12}+8m_tD_{25}-8m_tD_{26} \tag{C78}$$

$$f_{14}^{B_3} = -4m_tD_{11}+8m_tD_{12}-4m_tD_{13}+4m_tD_{24}-4m_tD_{25}$$
$$+\epsilon\left(-4m_tD_{22}+4m_tD_{24}-4m_tD_{25}+4m_tD_{26}\right) \tag{C79}$$

$$f_{15}^{B_3} = -4m_tD_{11}+4m_tD_{12}-8m_tD_{21}+8m_tD_{24} \tag{C80}$$

$$f_{16}^{B_3} = 4m_tD_{21}-4m_tD_{24}+\epsilon\left(4m_tD_{21}+4m_tD_{22}-8m_tD_{24}\right) \tag{C81}$$

$$f_{17}^{B_3} = 8D_{23}-8D_{26}-8D_{38}+\epsilon\left(-8D_{23}+8D_{26}+8D_{38}-8D_{39}\right)+8D_{39} \tag{C82}$$

$$f_{18}^{B_3} = 16D_{12}-16D_{13}+8D_{22}+16D_{24}-16D_{25}-8D_{26}+8D_{36}-8D_{310}$$
$$+\epsilon\left(-8D_{22}+8D_{26}-8D_{36}+8D_{310}\right) \tag{C83}$$

$$f_{19}^{B_3} = 8D_{25}-8D_{26}+8D_{38}-8D_{310}+\epsilon\left(8D_{25}-8D_{26}-8D_{38}+8D_{310}\right) \tag{C84}$$

$$f_{20}^{B_3} = -8D_{22}+8D_{24}+8D_{34}-8D_{36}+\epsilon\left(8D_{22}-8D_{24}-8D_{34}+8D_{36}\right), \tag{C85}$$

where the arguments of the scalar function and tensor coefficients are $\left(\left(-p_t\right)^2,\left(-p_W\right)^2,p_b^2,p_g^2;s,t;0,m_t^2,0,0\right)=\left(m_t^2,m_W^2,0,0;s,t;0,m_t^2,0,0\right)$.

- Bubble correction S_1:

$$f_2^{S_3} = \frac{1}{t_1}\Big\{4B_0m_t+2B_1m_t+\epsilon\left(-2B_0m_t-2B_1m_t\right)\Big\}, \tag{C86}$$

$$f_6^{S_3} = \frac{1}{t_1^2}\Big\{16B_0m_t^2+4B_1\left(2m_t^2+t_1\right)+\epsilon\left(-8B_0m_t^2-4B_1\left(2m_t^2+t_1\right)\right)\Big\}, \tag{C87}$$

$$f_{12}^{S_3} = \frac{1}{t_1^2}\Big\{8B_0m_t^2+2B_1\left(2m_t^2+t_1\right)+\epsilon\left(-4B_0m_t^2-2B_1\left(2m_t^2+t_1\right)\right)\Big\}, \tag{C88}$$

where the arguments of the scalar function and tensor coefficients are $\left(\left(p_g-p_t\right)^2,m_t^2,0\right)=\left(t,m_t^2,0\right)$.

- Bubble correction S_2:

$$f_4^{S_4} = \frac{1}{s}\left\{4B_1 - 4B_1\epsilon\right\}, \tag{C89}$$

$$f_5^{S_4} = \frac{1}{s}\left\{4B_1 - 4B_1\epsilon\right\}, \tag{C90}$$

$$f_{11}^{S_4} = \frac{1}{s}\left\{4B_1\epsilon - 4B_1\right\}, \tag{C91}$$

$$f_{12}^{S_4} = \frac{1}{s}\left\{2B_1 - 2B_1\epsilon\right\}, \tag{C92}$$

where the arguments of the scalar function and tensor coefficients are $\left((p_g + p_b)^2, 0, 0\right) = (s, 0, 0)$.

APPENDIX D: DIVERGENCES OF THE FORM FACTORS

In this section we list out the divergent pieces of the form factors and and we further distinguish the UV divergence and the IR divergence. The former is written inside the square brackets, i.e. $[\cdots]$.

(1) The triangle loop V_1 only gives rise to the UV divergences,

$$f_6^{V_1} = 2f_{12}^{V_1} = \frac{2}{t_1}\left[\frac{1}{\epsilon_{UV}} - 2\right]. \tag{D1}$$

(2) The triangle loop V_2 exhibits both the UV and IR divergences,

$$f_6^{V_2} : \frac{1}{t_1}\left\{\left[\frac{6}{\epsilon_{UV}} - 4\right] - \frac{1}{\epsilon_{IR}^2} - \frac{4}{\epsilon_{IR}} - \frac{2}{\epsilon_{IR}}\ln\frac{-t_1}{m_t^2}\right\}, \tag{D2}$$

$$f_{12}^{V_2} : \frac{1}{t_1}\left\{\left[\frac{3}{\epsilon_{UV}} - 2\right] - \frac{1}{\epsilon_{IR}^2} - \frac{1}{\epsilon_{IR}} - \frac{2}{\epsilon_{IR}}\ln\frac{-t_1}{m_t^2}\right\}. \tag{D3}$$

(3) The triangle loop V_3 gives rise to both the UV and IR divergences,

$$f_3^{V_3} : \frac{1}{t_1}\left\{-\frac{4}{\epsilon_{IR}}\frac{m_t^2 - t}{m_W^2 - t}\left(-1 + \frac{m_t^2 - m_W^2}{m_W^2 - t}\ln\frac{-t_1}{m_t^2 - m_W^2}\right)\right\}, \tag{D4}$$

$$f_6^{V_3} : \frac{1}{t_1}\left\{\left[\frac{2}{\epsilon_{UV}} - 4\right] + \frac{4}{\epsilon_{IR}}\left(-1 + \frac{m_t^2 - m_W^2}{m_W^2 - t}\ln\frac{-t_1}{m_t^2 - m_W^2}\right)\right\}, \tag{D5}$$

$$f_{12}^{V_3} : \frac{1}{t_1}\left\{\left[\frac{1}{\epsilon_{UV}} - 2\right] + \frac{2}{\epsilon_{IR}}\left(-1 + \frac{m_t^2 - m_W^2}{m_W^2 - t}\ln\frac{-t_1}{m_t^2 - m_W^2}\right)\right\}. \tag{D6}$$

(4) The triangle loop V_1' give rise to both the UV and IR divergences,

$$f_3^{V_1'} \; : \; \frac{1}{s}\left\{\left[-\frac{2}{\epsilon_{UV}}+4\right]+\frac{4}{\epsilon_{IR}}\right\}, \tag{D7}$$

$$f_4^{V_1'} \; : \; \frac{1}{s}\left[\frac{2}{\epsilon_{UV}}-4\right], \tag{D8}$$

$$f_5^{V_1'} \; : \; \frac{1}{s}\left\{\left[\frac{2}{\epsilon_{UV}}-4\right]-\frac{4}{\epsilon_{IR}}\right\}, \tag{D9}$$

$$f_{11}^{V_1'} \; : \; \frac{1}{s}\left\{\left[-\frac{2}{\epsilon_{UV}}+4\right]+\frac{4}{\epsilon_{IR}}\right\}, \tag{D10}$$

$$f_{12}^{V_1'} \; : \; \frac{1}{s}\left\{\left[\frac{1}{\epsilon_{UV}}-2\right]-\frac{2}{\epsilon_{IR}}\right\}. \tag{D11}$$

(5) The triangle loop V_2' gives rise to both the UV and IR divergences,

$$f_3^{V_2'} \; : \; \frac{1}{s}\left\{\left[-\frac{6}{\epsilon_{UV}}+4\right]+\frac{4}{\epsilon_{IR}^2}+\frac{6}{\epsilon_{IR}}-\frac{4}{\epsilon_{IR}}\ln\frac{-u-t_1}{m_t^2}\right\}, \tag{D12}$$

$$f_4^{V_2'} \; : \; \frac{1}{s}\left\{\left[\frac{6}{\epsilon_{UV}}-4\right]-\frac{2}{\epsilon_{IR}^2}-\frac{6}{\epsilon_{IR}}+\frac{2}{\epsilon_{IR}}\ln\frac{-u-t_1}{m_t^2}\right\}, \tag{D13}$$

$$f_5^{V_2'} \; : \; \frac{1}{s}\left\{\left[\frac{6}{\epsilon_{UV}}-4\right]-\frac{4}{\epsilon_{IR}^2}-\frac{6}{\epsilon_{IR}}+\frac{4}{\epsilon_{IR}}\ln\frac{-u-t_1}{m_t^2}\right\}, \tag{D14}$$

$$f_{11}^{V_2'} \; : \; \frac{1}{s}\left\{\left[-\frac{6}{\epsilon_{UV}}+4\right]+\frac{4}{\epsilon_{IR}^2}+\frac{6}{\epsilon_{IR}}-\frac{4}{\epsilon_{IR}}\ln\frac{-u-t_1}{m_t^2}\right\}, \tag{D15}$$

$$f_{12}^{V_2'} \; : \; \frac{1}{s}\left\{\left[\frac{3}{\epsilon_{UV}}-2\right]-\frac{2}{\epsilon_{IR}^2}-\frac{3}{\epsilon_{IR}}+\frac{2}{\epsilon_{IR}}\ln\frac{-u-t_1}{m_t^2}\right\}. \tag{D16}$$

(6) The triangle loop V_3' contains only the UV divergences:

$$-f_3^{V_3'}=f_4^{V_3'}=f_5^{V_3'}=-f_{11}^{V_3'}=2f_{12}^{V_3'}=\frac{2}{s}\left[\frac{1}{\epsilon_{UV}}-2\right]. \tag{D17}$$

(7) The box loops $B_{1,2,3}$ only contain the IR divergences. B_1 gives rise to the following IR divergences:

$$f_3^{B_1} \; : \; -\frac{1}{\epsilon_{IR}}\frac{4}{t-m_W^2}\left\{1+\frac{m_t^2-m_W^2}{t-m_W^2}\ln\frac{-t_1}{m_t^2-m_W^2}\right\}, \tag{D18}$$

$$f_6^{B_1} \; : \; \frac{1}{t_1}\left\{-\frac{2}{\epsilon_{IR}^2}+\frac{4}{\epsilon_{IR}}\ln\frac{m_t^2-m_W^2-u}{m_t^2}+\frac{4}{\epsilon_{IR}}\frac{m_t^2-m_W^2}{t-m_W^2}\ln\frac{-t_1}{m_t^2-m_W^2}\right\}, \tag{D19}$$

$$f_{12}^{B_1} \; : \; \frac{1}{2}f_6^{B_1}. \tag{D20}$$

(8) B_2 gives rise to the following divergences:

$$f_3^{B_2}=-f_5^{B_2}=f_{11}^{B_2}=-2f_{12}^{B_2} \; : \; \frac{1}{s}\left\{\frac{2}{\epsilon_{IR}^2}-\frac{4}{\epsilon_{IR}}\ln\frac{m_t^2-m_W^2-u}{m_t^2}\right\}, \tag{D21}$$

$$f_4^{B_2} \; : \; \frac{1}{s}\left\{\frac{-2}{\epsilon_{IR}^2}+\frac{4}{\epsilon_{IR}}\ln\frac{m_t^2-m_W^2-u}{m_t^2}-\frac{4}{\epsilon_{IR}}\right\}. \tag{D22}$$

(9) B_3 gives rise to the following divergences:

$$f_3^{B_3} : \frac{1}{s}\left\{\frac{4}{\epsilon_{IR}^2}+\frac{2}{\epsilon_{IR}}-\frac{4}{\epsilon_{IR}}\ln\frac{-t_1}{m_t^2}-\frac{4}{\epsilon_{IR}}\frac{m_t^2-m_W^2}{t-m_W^2}\ln\frac{-t_1}{m_t^2-m_W^2}\right\} - \frac{4}{\epsilon_{IR}\,(t-m_W^2)}, \tag{D23}$$

$$f_4^{B_3} : \frac{1}{s}\left\{-\frac{4}{\epsilon_{IR}^2}-\frac{2}{\epsilon_{IR}}+\frac{4}{\epsilon_{IR}}\ln\frac{-t_1}{m_t^2}+\frac{2}{\epsilon_{IR}}\ln\frac{s}{m_t^2}\right\}, \tag{D24}$$

$$f_5^{B_3} : \frac{1}{s}\left\{-\frac{2}{\epsilon_{IR}^2}-\frac{2}{\epsilon_{IR}}+\frac{4}{\epsilon_{IR}}\ln\frac{-t_1}{m_t^2}\right\}, \tag{D25}$$

$$f_6^{B_3} : \frac{1}{t_1}\left\{-\frac{5}{\epsilon_{IR}^2}+\frac{4}{\epsilon_{IR}}\ln\frac{s}{m_t^2}+\frac{4}{\epsilon_{IR}}\frac{m_t^2-m_W^2}{t-m_W^2}\ln\frac{-t_1}{m_t^2-m_W^2}+\frac{2}{\epsilon_{IR}}\ln\frac{-t_1}{m_t^2}\right\}, \tag{D26}$$

$$f_{11}^{B_3} : \frac{1}{s}\left\{\frac{2}{\epsilon_{IR}^2}+\frac{2}{\epsilon_{IR}}-\frac{4}{\epsilon_{IR}}\ln\frac{-t_1}{m_t^2}\right\}, \tag{D27}$$

$$f_{12}^{B_3} : \frac{1}{s}\left\{-\frac{1}{\epsilon_{IR}^2}-\frac{1}{\epsilon_{IR}}+\frac{2}{\epsilon_{IR}}\ln\frac{-t_1}{m_t^2}\right\} + \frac{1}{t_1}\left\{-\frac{2}{\epsilon_{IR}^2}-\frac{1}{\epsilon_{IR}}+\frac{2}{\epsilon_{IR}}\ln\frac{s}{m_t^2}+\frac{2}{\epsilon_{IR}}\frac{m_t^2-m_W^2}{t-m_W^2}\ln\frac{-t_1}{m_t^2-m_W^2}\right\}. \tag{D28}$$

(10) The bubble loops $S_{1,2}$ only contain the UV divergences. S_1 gives rise to the following divergences:

$$f_2^{S_1} : \frac{m_t}{t_1}\left[\frac{3}{\epsilon_{UV}}-1\right], \tag{D29}$$

$$f_6^{S_1} : \frac{2}{t_1}\left[\frac{1}{\epsilon_{UV}}\frac{6m_t^2}{t_1}-\frac{1}{\epsilon_{UV}}-\frac{2m_t^2}{t_1}+1\right], \tag{D30}$$

$$f_{12}^{S_1} : \frac{1}{t_1}\left[\frac{1}{\epsilon_{UV}}\frac{6m_t^2}{t_1}-\frac{1}{\epsilon_{UV}}-\frac{2m_t^2}{t_1}+1\right], \tag{D31}$$

while S_2 gives rise to the following divergences:

$$f_3^{S_2}=-f_4^{S_2}=-f_5^{S_2}=f_{11}^{S_2}=-2f_{12}^{S_2}=\frac{2}{s}\left[\frac{1}{\epsilon_{UV}}-1\right]. \tag{D32}$$

[1] T. Tait and C.-P. Yuan, hep-ph/9710372 (1997), hep-ph/9710372.

[2] S. Dawson, Nucl. Phys. **B249**, 42 (1985).

[3] S. S. D. Willenbrock and D. A. Dicus, Phys. Rev. **D34**, 155 (1986).

[4] C.-P. Yuan, Phys. Rev. **D41**, 42 (1990).

[5] G. A. Ladinsky and C.-P. Yuan, Phys. Rev. **D43**, 789 (1991).

[6] S. Cortese and R. Petronzio, Phys. Lett. **B253**, 494 (1991).

[7] R. K. Ellis and S. J. Parke, Phys. Rev. **D46**, 3785 (1992).

[8] D. O. Carlson and C.-P. Yuan, Phys. Lett. **B306**, 386 (1993).

[9] G. Bordes and B. van Eijk, Nucl. Phys. **B435**, 23 (1995).

[10] T. Stelzer and S. Willenbrock, Phys. Lett. **B357**, 125 (1995), hep-ph/9505433.

[11] A. P. Heinson, A. S. Belyaev, and E. E. Boos, Phys. Rev. **D56**, 3114 (1997), hep-ph/9612424.

[12] M. C. Smith and S. Willenbrock, Phys. Rev. **D54**, 6696 (1996), hep-ph/9604223.

[13] S. Mrenna and C.-P. Yuan, Phys. Lett. **B416**, 200 (1998), hep-ph/9703224.

[14] T. Stelzer, Z. Sullivan, and S. Willenbrock, Phys. Rev. **D56**, 5919 (1997), hep-ph/9705398.

[15] S. Moretti, Phys. Rev. **D56**, 7427 (1997), hep-ph/9705388.

[16] T. Stelzer, Z. Sullivan, and S. Willenbrock, Phys. Rev. **D58**, 094021 (1998), hep-ph/9807340.

[17] A. S. Belyaev, E. E. Boos, and L. V. Dudko, Phys. Rev. **D59**, 075001 (1999), hep-ph/9806332.

[18] T. M. P. Tait, Phys. Rev. **D61**, 034001 (2000), hep-ph/9909352.

[19] A. Belyaev and E. Boos, Phys. Rev. **D63**, 034012 (2001), hep-ph/0003260.

[20] T. Tait and C.-P. Yuan, Phys. Rev. **D63**, 014018 (2001), hep-ph/0007298.

[21] M. Beccaria, G. Macorini, F. M. Renard, and C. Verzegnassi, Phys. Rev. **D74**, 013008 (2006), hep-ph/0605108.

[22] M. Beccaria et al. (2007), arXiv:0705.3101 [hep-ph].

[23] N. Kidonakis, Phys. Rev. **D74**, 114012 (2006), hep-ph/0609287.

[24] N. Kidonakis, Phys. Rev. **D75**, 071501 (2007), hep-ph/0701080.

[25] Q.-H. Cao, J. Wudka, and C. P. Yuan, Phys. Lett. **B658**, 50 (2007), arXiv:0704.2809 [hep-ph].

[26] C. E. Gerber et al. (TeV4LHC-Top and Electroweak Working Group) (2007), arXiv:0705.3251 [hep-ph].

[27] B. W. Harris, E. Laenen, L. Phaf, Z. Sullivan, and S. Weinzierl, Phys. Rev. **D66**, 054024

(2002), hep-ph/0207055.

[28] S. Zhu, Phys. Lett. **B524**, 283 (2002).

[29] J. Campbell, R. K. Ellis, and F. Tramontano, Phys. Rev. **D70**, 094012 (2004), hep-ph/0408158.

[30] Q.-H. Cao, R. Schwienhorst, and C. P. Yuan, Phys. Rev. **D71**, 054023 (2005), hep-ph/0409040.

[31] Q.-H. Cao and C. P. Yuan, Phys. Rev. **D71**, 054022 (2005), hep-ph/0408180.

[32] Z. Sullivan, Phys. Rev. **D70**, 114012 (2004), hep-ph/0408049.

[33] Q.-H. Cao, R. Schwienhorst, R. Brock, and C.-P. Yuan (in preparation).

[34] S. Frixione, E. Laenen, P. Motylinski, and B. R. Webber, JHEP **03**, 092 (2006), hep-ph/0512250.

[35] J. Campbell and F. Tramontano, Nucl. Phys. **B726**, 109 (2005), hep-ph/0506289.

[36] T. Kinoshita, J. Math. Phys. **3**, 650 (1962).

[37] T. D. Lee and M. Nauenberg, Phys. Rev. **133**, B1549 (1964).

[38] F. Gutbrod, G. Kramer, and G. Schierholz, Z. Phys. **C21**, 235 (1984).

[39] H. Baer, J. Ohnemus, and J. F. Owens, Phys. Rev. **D40**, 2844 (1989).

[40] F. Aversa, M. Greco, P. Chiappetta, and J. P. Guillet, Phys. Rev. Lett. **65**, 401 (1990).

[41] W. T. Giele and E. W. N. Glover, Phys. Rev. **D46**, 1980 (1992).

[42] W. T. Giele, E. W. N. Glover, and D. A. Kosower, Nucl. Phys. **B403**, 633 (1993), hep-ph/9302225.

[43] S. Keller and E. Laenen, Phys. Rev. **D59**, 114004 (1999), hep-ph/9812415.

[44] R. K. Ellis, D. A. Ross, and A. E. Terrano, Nucl. Phys. **B178**, 421 (1981).

[45] S. D. Ellis, Z. Kunszt, and D. E. Soper, Phys. Rev. **D40**, 2188 (1989).

[46] S. Bethke, Z. Kunszt, D. E. Soper, and W. J. Stirling, Nucl. Phys. **B370**, 310 (1992).

[47] M. L. Mangano, P. Nason, and G. Ridolfi, Nucl. Phys. **B373**, 295 (1992).

[48] S. Frixione, Z. Kunszt, and A. Signer, Nucl. Phys. **B467**, 399 (1996), hep-ph/9512328.

[49] S. Catani and M. H. Seymour, Phys. Lett. **B378**, 287 (1996), hep-ph/9602277.

[50] S. Catani and M. H. Seymour, Nucl. Phys. **B485**, 291 (1997), hep-ph/9605323.

[51] A. Brandenburg and P. Uwer, Nucl. Phys. **B515**, 279 (1998), hep-ph/9708350.

[52] G. Passarino and M. J. G. Veltman, Nucl. Phys. **B160**, 151 (1979).

[53] G. 't Hooft and M. J. G. Veltman, Nucl. Phys. **B153**, 365 (1979).

[54] R. K. Ellis and G. Zanderighi (2007), arXiv:0712.1851 [hep-ph].

[55] A. Bassetto, M. Ciafaloni, and G. Marchesini, Phys. Rept. **100**, 201 (1983).

[56] F. A. Berends and W. T. Giele, Nucl. Phys. **B313**, 595 (1989).

[57] W. Beenakker, H. Kuijf, W. L. van Neerven, and J. Smith, Phys. Rev. **D40**, 54 (1989).